

An integrated theoretical study on natural alkaloids as SARS-CoV-2 main protease inhibitors: A step toward discovery of potential drug candidate with anti-covid-19 activity

Shagufta Parveen¹, Laiba Shahbaz¹, Nusrat Shafiq^{1*}, Maryam Rashid¹, Mohamed Mohany², Mingkun Zhu^{3,4}

¹Synthetic and Natural Products Discovery (SNPD) Laboratory, Department of Chemistry, Government College Women University Faisalabad-38000, Pakistan

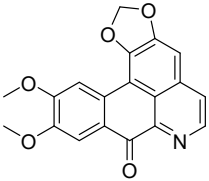
²Department of Pharmacology and Toxicology, College of Pharmacy, King Saud University, P.O. Box 55760, Riyadh 11451, Saudi Arabia.
mmohany@ksu.edu.sa

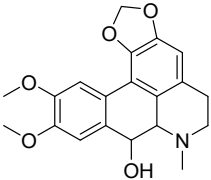
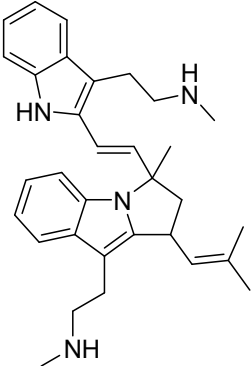
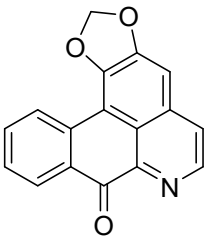
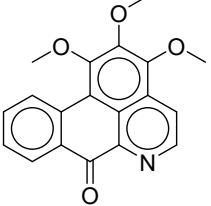
³Jiangsu Key Laboratory of Sericultural Biology and Animal Biotechnology, School of Biotechnology, Jiangsu University of Science and Technology, Zhenjiang 212100, China.
mkzhu085@just.edu.cn

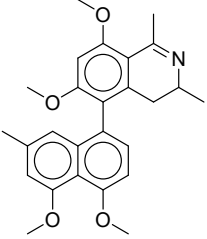
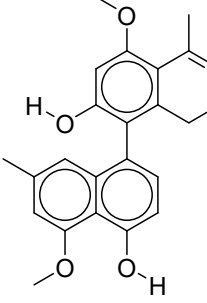
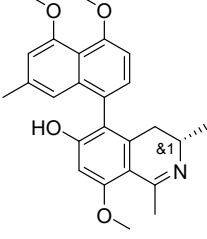
⁴Key Laboratory of Silkworm and Mulberry Genetic Improvement, Ministry of Agriculture and Rural Affairs, The Sericultural Research Institute, Chinese Academy of Agricultural Sciences, Zhenjiang 212100, China

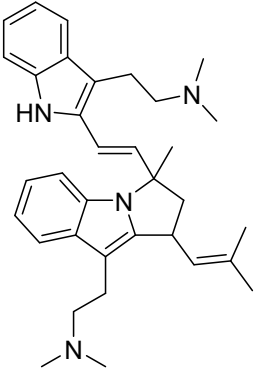
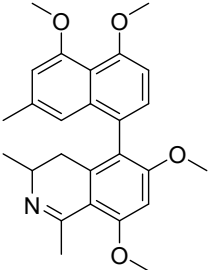
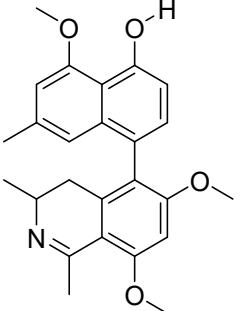
Corresponding Authors: Dr. Nusrat Shafiq, Assistant Professor
Corresponding Address: dr.nusratshafiq@gcwuf.edu.pk; gqumarin@gmail.com
ORCID: orcid.org/0000-0002-3270-4227

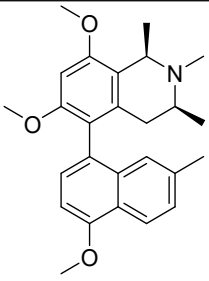
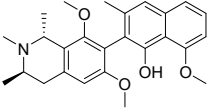
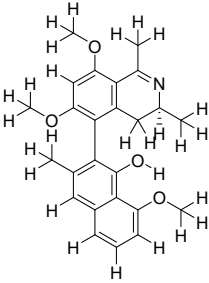
Table S-1: Dataset of antiparasitic natural alkaloids with their IC₅₀ values and their sources

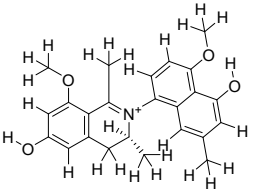
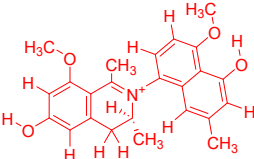
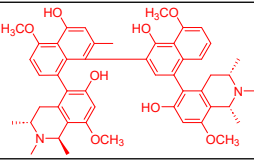
S No	Name	Formula	Smiles	Activity	Structure	IC ₅₀ /EC ₅₀	Source	Reference
						μM / nm / μg/mL / mM		
1	Dicentrinone	C ₁₉ H ₁₃ NO ₅	<chem>COC1=C(C=C2C(=C1)C3=C4C(=CC5=C3OC(O5)C=CN=C4C2=O)OC</chem>	Against free trypomastigotes of the Ystrain of <i>T.cruzi</i>		16.4 μM	fresh leaves of <i>Ocotea puberula</i>	(Fernández <i>et al.</i> , 2021a).

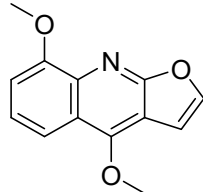
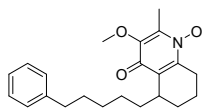
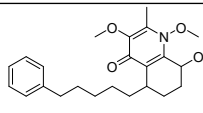
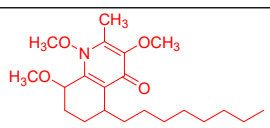
2	Duguetine	C ₂₀ H ₂₁ NO ₅	<chem>CN1CCC2=CC3=C(C4=C2C1C(C5=CC(=C(C=C54)OC)OC)O)OCO3</chem>	Against free trypomastigotes of the Ystrain of <i>T. cruzi</i>		9.32 μM	fresh leaves of <i>Ocotea puberula</i>	(Fernández <i>et al.</i> , 2021a).
3	Flinderole A	C ₃₂ H ₄₀ N ₄	<chem>CC(=CC1CC(N2C1=C(C3=CC=CC=C32)CCN(C)C)C=CC4=C(C5=CC=CC=C5N4)CCNC)C</chem>	against <i>P. falciparum</i> 3D7 strain		0.75 μM	Australian species <i>Flindersia acuminata</i>	(Fernandez <i>et al.</i> , 2010).
4	Liriodenine	C ₁₇ H ₉ NO ₃	<chem>C1OC2=C(O1)C3=C4C(=C2)C=CN=C4C(=O)C5=CC=CC=C53</chem>	against the trypomastigote of <i>T. cruzi</i>		14.5 μM	<i>Annona foetida</i>	(Fernández <i>et al.</i> , 2021a).
5	O-methylmoschatoline	C ₁₉ H ₁₅ NO ₄	<chem>COc1c2ccnc3c2c(c(c1OC)OC)-c4ccccc4C3=O</chem>	against the trypomastigote of <i>T. cruzi</i>		11.83 μM	<i>Annona foetida</i>	(Fernández <i>et al.</i> , 2021a).

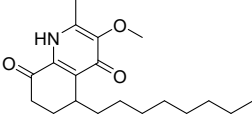
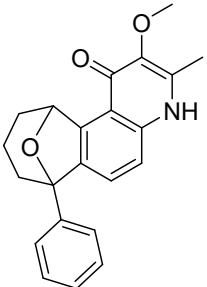
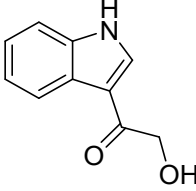
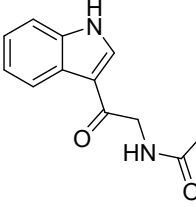
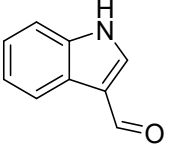
6	ancistroealaine A	C ₂₆ H ₂₉ NO ₄	<chem>Cc1cc2c(ccc(c2c(c1)OC)OC)c3c(cc(c4c3CC(N=C4C)C)OC)OC</chem>	against trypomastigotes (Tulahuen C4, L6 cells)		5.6 μM	isolated from lianas from the Ancistrocladus genus	(Fernández <i>et al.</i> , 2021a).
7	6,5'-O,O-didemethylancistroealaine A	C ₂₄ H ₂₅ NO ₄	<chem>Cc1c(cc(OC)c2c1c(c3c(CC(C)N=C4C)c4c(OC)cc3O[H])ccc2O[H])</chem>	against trypomastigotes (Tulahuen C4, L6 cells)		16.3 μM	isolated from lianas from the Ancistrocladus genus	(Fernández <i>et al.</i> , 2021a).
8	6-O-demethylancistroealaine A	C ₂₅ H ₂₇ NO ₄	<chem>OC1=C(C2=C3C=C(C)C=C(OC)C3=C(OC)C=C2)C(C[C@H](C)N=C4C)=C4C(OC)=C1</chem>	against trypomastigotes (Tulahuen C4, L6 cells)		25.9 μM	isolated from lianas from the Ancistrocladus genus	(Fernández <i>et al.</i> , 2021a).

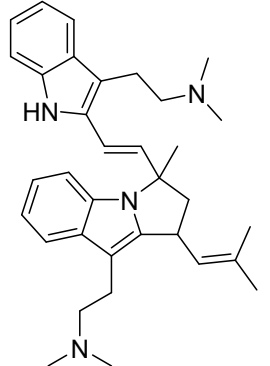
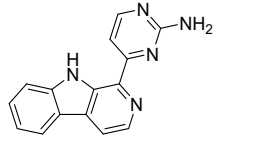
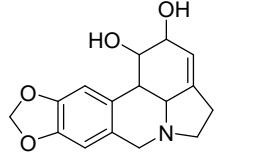
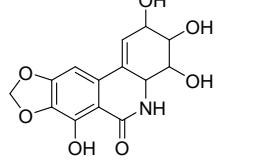
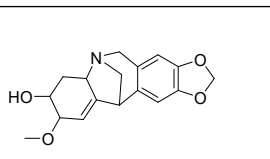
9	Flinderole B	C ₃₄ H ₄₄ N ₄	<chem>CC(=CC1CC(N2C1=C(C3=CC=CC=C3)CCN(C)C)(C)C=CC4=C(C5=CC=C(C=C5N4)CCN(C)C)C</chem>	against <i>P. falciparum</i> 3D7 strain		0.21 μM	<i>F. amboinensis</i>	(Fernandez <i>et al.</i> , 2010).
10	ancistrotanzanine B	C ₂₆ H ₂₉ N ₄ O ₄	<chem>CC1CC2=C(C(=CC(=C2C(=N1)C)OC)OC)C3=C4C=C(C=C(C4=C(C=C3)OC)OC)C</chem>	against β-gal Tulahuen trypomastigotes		3.58 μM	isolated from lianas from the <i>Ancistrocladus</i> genus	(Fernández <i>et al.</i> , 2021a).
11	ancistectorine D	C ₂₅ H ₂₇ N ₄ O ₄	<chem>CC1CC2=C(C3=C4C=C(C)C=C(OC)C4=C(O[H])C=C3)C(OC)=CC(OC)=C2C(C)=N1</chem>	against <i>T. cruzi</i>		4.439 μM	isolated from lianas from the <i>Ancistrocladus</i> genus	(Fernández <i>et al.</i> , 2021a).

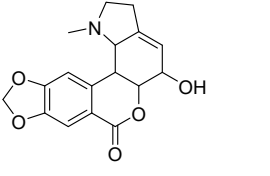
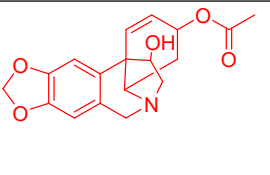
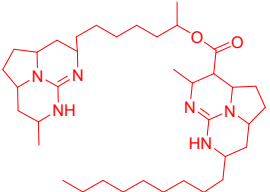
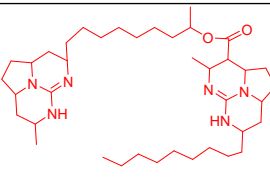
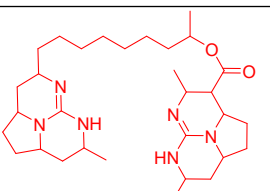
12	5-epi-4'-O-demethylancistrobertsonine C	C ₂₆ H ₃₁ NO ₄	<chem>CC1=CC=C2C(OC)=CC=C(C3=C(OC)C=C(O)C4=C3C[C@H](C)N(C)[C@@H]4C)C2=C1</chem>	against T. cruzi		11.1 μM	isolated from lianas from the Ancistrocladus genus	(Fernández <i>et al.</i> , 2021a).
13	Ancistotectorine	C ₂₆ H ₃₁ NO ₄	<chem>COC1=CC=CC2=C(C(=O)=C12)C1=C(OC)C2=C(C[C@@H](C)N(C)[C@@H]2C)C=C1OC</chem>	against T. cruzi		10.2 μM	isolated from lianas from the Ancistrocladus genus	(Fernández <i>et al.</i> , 2021a).
14	.Ancistrotanzanine A	C ₂₅ H ₂₇ NO ₄	<chem>[H]OC1=C2C(OC([H]))([H])[H])=C([H])C([H])=C([H])C2=C([H])C(=C1C1=C(C(OC([H]))([H])[H])C([H])=C(OC([H]))([H])[H])C2=C1C([H])([H])[C@@]([H])([H]15)(N=C2C([H])([H])[H])C([H])([H])[H])C([H])([H])[H]</chem>	against T. cruzi		4.20 μM	isolated from lianas from the Ancistrocladus genus	(Fernández <i>et al.</i> , 2021a).
15	4'-O-demethylancistrocl	C ₂₅ H ₂₈ NO ₄	<chem>[H]OC1=C(C(C([H]))([H])[H])=</chem>	against Tulahuen C4		0.03μM	isolated from lianas from the	(Fernández <i>et al.</i> , 2021a).

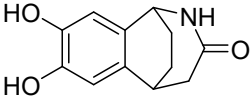
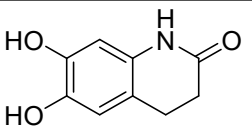
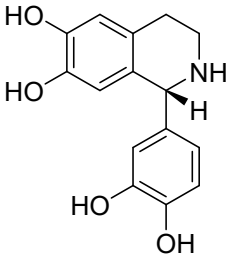
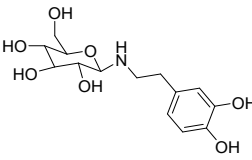
	adinium A		<chem>C(C2=C([N+]3=C(C([H])([H])[H])C4=C(C([H])([C@@]3(C([H])([H])([H])[H])C([H])=C(C([H])=C4OC([H])([H])[H])O[CH]C([H])=C(C(OC([H])([H])[H])=C12)[H])[H])</chem>	trypomastigotes of T. cruzi			Ancistrocladus genus	
16	6,4'-O-didemethylancistrocladinium A	C24H26NO4+	<chem>[H]OC1=C(C(C([H])([H])[H])=C(C2=C([N+]3=C(C([H])([H])[H])C4=C(C([H])([C@@]3(C([H])([H])([H])[H])C([H])=C(C([H])=C4OC([H])([H])[H])O[CH]C([H])=C(C(OC([H])([H])[H])=C12)[H])[H])</chem>	against Tulahuen C4 trypomastigotes of T. cruzi		6.0 μM	isolated from lianas from the Ancistrocladus genus	(Fernández <i>et al.</i> , 2021a).
17	Mbandakamine B2	C49H54N2O8	<chem>OC1=CC(C)=C(C2=CC(C3=C(O)C=C(OC)C4=C3C[C@H](C</chem>	against Tulahuen C4 trypomastigotes of T.		2.98 μM	isolated from lianas from the Ancistrocladus genus	(Fernández <i>et al.</i> , 2021a).

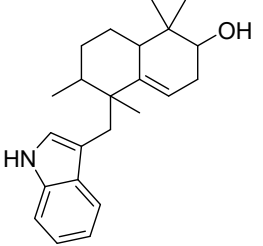
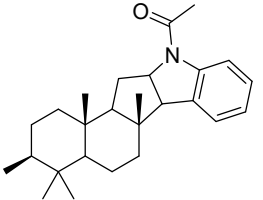
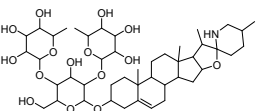
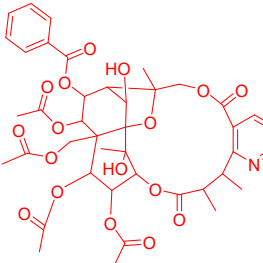
)N(C)[C@@H]4C)=C(C=CC=C5OC)C5=C2O)C6=C(C7=C(O)C=C(OC)C8=C7C[C@@H](C)N(C)[C@@H]8C)C=CC(OC)=C61	cruzi				
18	γ -fagarine	C ₁₃ H ₁₁ NO ₃	COC1=CC=CC2=C1N=C1OC=CC1=C2OC	against epimastigote sof the Y strain of T.cruzi		33.4 μ M	isolated from lianas from the Ancistrocladus genus	(Fernández <i>et al.</i> , 2021a).
19	Waltherione G	C ₂₃ H ₃₁ NO ₃	CC1=C(C(=O)C2=C(N1OC)C3=CC=CC=C3)OC	against amastigotes (Tuluhaen C2C4 (LacZ))		0.02 μ M	aerial parts and roots of Waltheria indicas	(Fernández <i>et al.</i> , 2021a).
20	Waltheriones H	C ₂₄ H ₃₃ NO ₄	CC1=C(C(=O)C2=C(N1OC)C3=CC=CC=C3)OC	against amastigotes (Tuluhaen C2C4 (LacZ))		0.04 μ M	aerial parts and roots of Waltheria indicas	(Fernández <i>et al.</i> , 2021a).
21	Waltheriones K	C ₂₁ H ₃₅ NO ₄	CCCCCCCCC1CCC(C2=C1C(=O)C=C(N2O)C)OC	against amastigotes (Tuluhaen C2C4 (LacZ))		0.04 μ M	aerial parts and roots of Waltheria indicas	(Fernández <i>et al.</i> , 2021a).

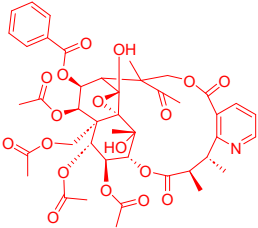
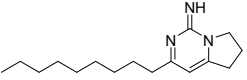
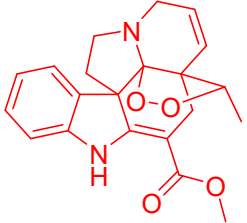
22	Antidesmone	C ₁₉ H ₂₉ NO ₃	CCCCCCCCC1 CCC(=O)C2=C 1C(=O)C(=C(N 2)C)OC	against amastigotes (Tuluhaen C2C4 (LacZ))		0.062 μM	aerial parts and roots of <i>Waltheria indicas</i>	(Fernández <i>et al.</i> , 2021a).
23	Waltherione C	C ₂₂ H ₂₁ NO ₃	CC1=C(C(=O) C2=C(N1)C=C C3=C2C4CCC C3(O4)C5=CC =CC=C5)OC	against amastigotes (Tuluhaen C2C4 (LacZ))		1.93 μM	aerial parts and roots of <i>Waltheria indicas</i>	(Fernández <i>et al.</i> , 2021a).
24	3- hydroxyacetylindol e	C ₁₀ H ₉ NO ₂	C1=CC=C2C(= C1)C(=CN2)C(=O)CO	amastigotes (Tulahuén β- gal)		20.6 μM	black coral <i>Antipathes</i> sp.	(Fernández <i>et al.</i> , 2021a).
25	N-acetyl-β- oxotryptamine	C ₁₂ H ₁₂ N ₂ O ₂	CC(=O)NCC(= O)C1=CNC2=C C=CC=C12	amastigotes (Tulahuén β- gal)		19.4 μM	black coral <i>Antipathes</i> sp.	(Fernández <i>et al.</i> , 2021a).
26	3-formylindole	C ₉ H ₇ NO	C1=CC=C2C(= C1)C(=CN2)C= O	amastigotes (Tulahuén β- gal)		26.9 μM	black coral <i>Antipathes</i> sp.	(Fernández <i>et al.</i> , 2021a).

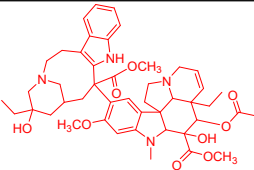
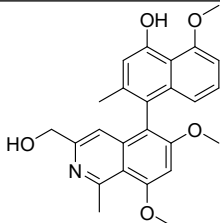
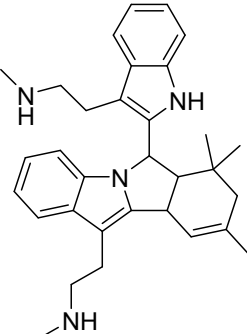
27	Flinderole C	C ₃₄ H ₄₄ N ₄	<chem>CC(=CC1CC(N2C1=C(C3=CC=CC=C3)CCN(C)C)(C)C=CC4=C(C5=CC=C(C=C5N4)CCN(C)C)C</chem>	against <i>P. falciparum</i> FCR3 strain		0.36 μM	<i>F. amboinensis</i>	(Fernández <i>et al.</i> , 2021b).
28	Annomontine	C ₁₅ H ₁₁ N ₅	<chem>C1=CC=C2C(=C1)C3=C(N2)C(=NC=C3)C4=NC(=NC=C4)N</chem>	trypomastigotes (Y strain) of <i>T. cruzi</i>		16.08 μM	branches of <i>Annona foetida</i>	(Fernández <i>et al.</i> , 2021a).
29	Lycorine	C ₁₆ H ₁₇ NO ₄	<chem>C1CN2CC3=C4C=C(C=C3C5C2C1=CC(C5O)O)OCO4</chem>	anti- <i>T. cruzi</i> activity		0.70 μM	isolated from extracts of different <i>Narcissus</i> species	(Fernández <i>et al.</i> , 2021a).
30	Narciclasine	C ₁₄ H ₁₃ NO ₇	<chem>C1OC2=C(O1)C(=C3C(=C2)C4=CC(C(C4N3=O)O)O)O</chem>	anti- <i>T. cruzi</i> activity		0.49 μM	isolated from extracts of different <i>Narcissus</i> species	(Fernández <i>et al.</i> , 2021a).
31	Montanine	C ₁₇ H ₁₉ NO ₄	<chem>COC1C=C2C(C1O)N3CC2C4=CC5=C(C=C4C3)OCO5</chem>	anti- <i>T. cruzi</i> activity		1.99 μM	isolated from extracts of different <i>Narcissus</i> species	(Fernández <i>et al.</i> , 2021a).

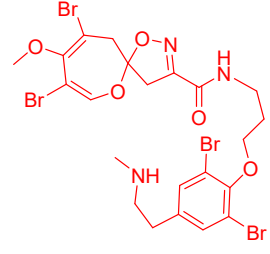
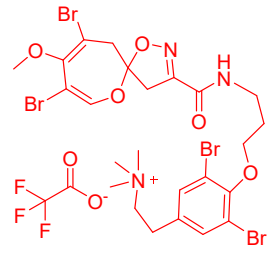
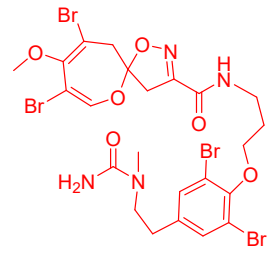
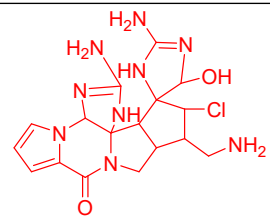
32	Hippeastrine	<u>C₁₇H₁₇NO₅</u>	CN1CCC2=CC(C3C(C21)C4=C5=C(C=C4C(=O)O3)OCO5)O	anti-T. cruzi activity		3.31 μM	isolated from extracts of different Narcissus species	(Fernández <i>et al.</i> , 2021a).
33	3-O-acetylhamayne	<u>C₁₈H₁₉NO₅</u>	CC(=O)OC1CC2C3(C=C1)C(CN2CC4=CC5=C(C=C34)OCO5)O	against the amastigote form (Tulahuen β-gal C2C4 strain)		25.2 μM	fresh bulbs of Crinum amabile	(Fernández <i>et al.</i> , 2021a).
34	Batzelladine F	<u>C₃₇H₆₄N₆O₂</u>	CCCCCCCCC1CC2CCC3N2C(=NC(C3C(=O)OC(C)CCCCC4CC5CCC6N5C(=N4)NC(C6)C)C)N1	trypomastigotes(Ystrain) of T.cruzi		5 μM	marine sponge Monanchora arbuscula	(Fernández <i>et al.</i> , 2021a).
35	Batzelladine L	<u>C₃₉H₆₈N₆O₂</u>	CCCCCCCCC1CC2CCC3N2C(=NC(C3C(=O)OC(C)CCCCC4CC5CC6N5C(=N4)NC(C6)C)C)N1	trypomastigotes(Ystrain) of T.cruzi		2 μM	marine sponge Monanchora arbuscula	(Fernández <i>et al.</i> , 2021a).
36	nor-batzelladine L	<u>C₃₈H₆₆N₆O₂</u>	CCCCCCCCC1CC2CCC3N2C(=NC(C3C(=O)OC(C)CCCCC4CC5CCC	trypomastigotes(Ystrain) of T.cruzi		7 μM	marine sponge Monanchora arbuscula	(Fernández <i>et al.</i> , 2021a).

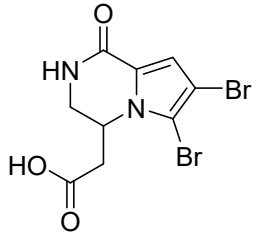
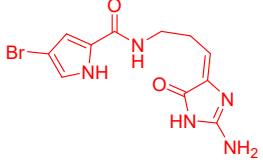
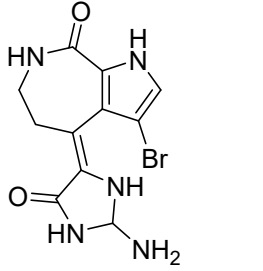
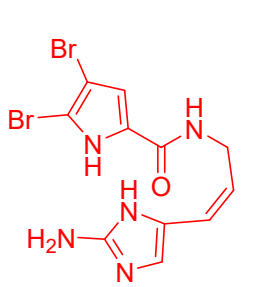
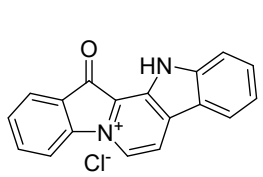
			6N5C(=N4)NC(C6)C)N1					
37	Alternamide A	C12H13NO3	<chem>O=C1CC2C3=CC(O)=C(O)C=C3C(CC2)N1</chem>	Against free trypomastigotes (Ystrain) of <i>T.cruzi</i>		0.61 μM	aerial parts of <i>Alternanthera littoralis</i>	(Fernández <i>et al.</i> , 2021a).
38	Alternamide B	C9H9NO3	<chem>O=C1CCC2=C(C(O)=C(O)C=C2)N1</chem>	Against free trypomastigotes (Ystrain) of <i>T.cruzi</i>		10 μM	aerial parts of <i>Alternanthera littoralis</i>	(Fernández <i>et al.</i> , 2021a).
39	Alternamine A	C15H15NO4	<chem>OC1=C(O)C=C([C@](C2=CC(O)=C(O)C=C2)([H])NCC3)C3=C1</chem>	Against free trypomastigotes (Ystrain) of <i>T.cruzi</i>		0.23 μM	aerial parts of <i>Alternanthera littoralis</i>	(Fernández <i>et al.</i> , 2021a).
40	Alternamine B	C14H21NO7	<chem>OC1=CC(CCN[C@@H]2O[C@@H](CO)[C@@H](O)C(O)[C@@H]2O)=CC=C1O</chem>	Against free trypomastigotes (Ystrain) of <i>T.cruzi</i>		0.82 μM	aerial parts of <i>Alternanthera littoralis</i>	(Fernández <i>et al.</i> , 2021a).

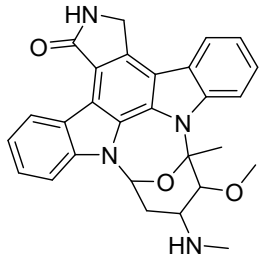
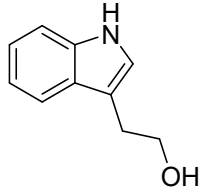
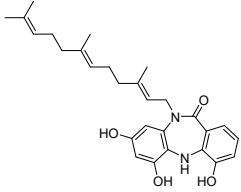
41	Polyalthenol	<u>C₂₃H₃₁NO</u>	CC1CCC2C(=C CC(C2(C)C)O) C1(C)CC3=CN C4=CC=CC=C 43	against trypomastig otes (Tulahuen strain) of T.cruzi		8.4 μM	Root bark of Greenwayodendr on suaveolens	(Fernández <i>et al.</i> , 2021a).
42	N-acetyl- polyveoline	C ₂₆ H ₃₇ NO	CC1(C)[C@@ H](C)CC[C@@]2(C)C1CC[C@]3(C)C2CC4C3 C(C=CC=C5)= C5N4C(C)=O	against trypomastig otes (Tulahuen strain)		8.4 μM	Root bark of Greenwayodendr on suaveolens	(Fernández <i>et al.</i> , 2021a).
43	Solamargine	<u>C₄₅H₇₃NO₁₅</u>	CC1CCC2(C(C 3C(O2)CC4C3(CCC5C4CC=C 6C5(CCC(C6)O C7C(C(C(C(O7)CO)OC8C(C(C (C(O8)C)O)O O)O)OC9C(C(C(C(O9)C)O)O)O)C)C)NC1	against epimastigote s of the Y strain of T.cruzi		17.63μ M	isolated from Solanum palinacanthum	(Fernández <i>et al.</i> , 2021a).
44	Ilicifoliunines A	C ₄₁ H ₄₇ NO ₁₇	CC1C(C(=O)O C2C(C(C3(C(C (C4C(C3(C2(C O)OC4(COC(= O)C5=C1N=CC =C5)C)O)OC(= O)C6=CC=CC= C6)OC(=O)C)C OC(=O)C)OC(against the epimastigote s (Y strain) of T.cruzi		27.7 μM	root bark of Maytenus ilicifolia	(Fernández <i>et al.</i> , 2021a).

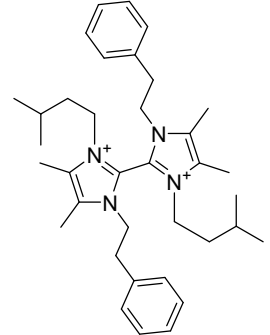
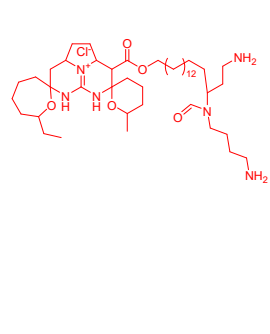
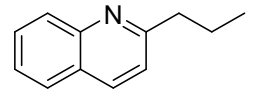
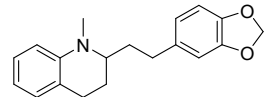
			<chem>=O)C)OC(=O)C)C</chem>					
45	Aquifoliunine E-I	$C_{43}H_{49}NO_{18}$	<chem>C[C@@H]1[C@@H](C)C(=O)O[C@@H]2[C@@H](OC(C)=O)[C@H](OC(C)=O)[C@@]3(COC(C)=O)[C@@H](OC(C)=O)[C@@H](OC(C)=O)C4=CC=CC=C4)[C@H]4[C@H](OC(C)=O)[C@@]3(O[C@]4(C)COC(=O)C3=C1N=CC=C3)[C@@]2(C)O</chem>	against the epimastigotes (Y strain) of T.cruzi		41.9 μ M	root bark of <i>Maytenus ilicifolia</i>	(Fernández <i>et al.</i> , 2021a).
46	Monalidine A	$C_{16}H_{27}N_3$	<chem>CCCCCCCCC1=NC(=N)N2CCCC2=C1</chem>	against free trypomastigotes (Y strain) of T.cruzi		8 μ M	isolated from the marine sponge <i>Monanchora arbuscula</i>	(Fernández <i>et al.</i> , 2021a).
47	Catharoseumine	$C_{21}H_{22}N_2O_4$	<chem>CC1C23CC(=C4C5(C2(N(CC5)CC=C3)OO1)C6=CC=CC=C6N4)C(=O)OC</chem>	against protozoan parasite falcipain-2		4.06 μ M	whole plant of <i>C. roseus</i>	(Almagro <i>et al.</i> , 2015).

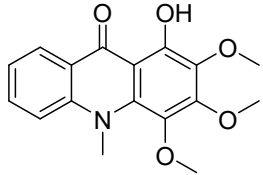
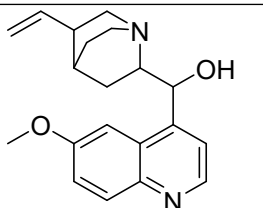
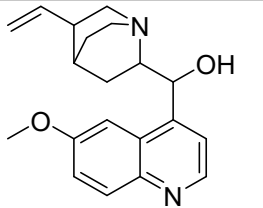
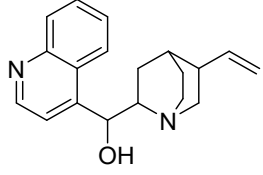
48	Vinblastine	$C_{46}H_{58}N_4O_9$	<chem>CCC1(CC2CC(C3=C(CCN(C2)C1)C4=CC=CC=C4N3)(C5=C(C=C6C(=C5)C78CCN9C7C(C=CC9)(C(C(C8N6C)(C(=O)OC)O)OC(=O)C)C)OC)C(=O)OC)O</chem>	against Trypanosoma cruzi		15 μ M	whole plant of <i>C. roseus</i>	(Dey <i>et al.</i> , 2020).
49	ancistrobenomine A	$C_{25}H_{25}NO_5$	<chem>COC1=CC=CC2=C(C(C)=CC(O)=C12)C1=C2C=C(CO)N=C(C)C2=C(OC)C=C1OC</chem>	against T. cruzi		11.45 μ M	isolated from lianas from the <i>Ancistrocladus</i> genus	(Dey <i>et al.</i> , 2020).
50	Isoborreverine	$C_{32}H_{40}N_4$	<chem>CC1=CC2C(C(N3C2=C(C4=C(C=CC=C43)CCNC)C5=C(C6=CC=CC=C6N5)CCNC)C(C1)(C)C</chem>	against P. falciparum 3D7 strain		0.24 μ M	Australian species <i>Flindersia acuminata</i>	(Fernandez <i>et al.</i> , 2010).
51	psammaplysin F	$C_{22}H_{25}Br_4N_3O_5$	<chem>CNCCC1=CC(=C(C(=C1)Br)OCCCNC(=O)</chem>	against T. cruzi		5.6 μ M	<i>Hyatella</i> sp.	(Tempone <i>et al.</i> , 2021).

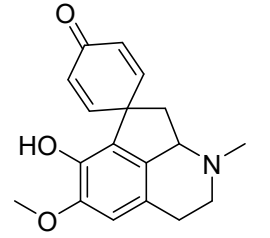
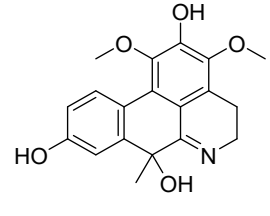
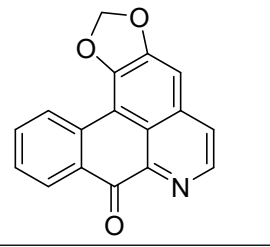
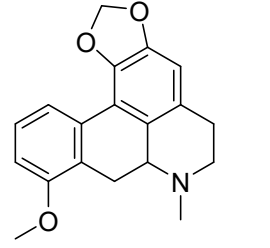
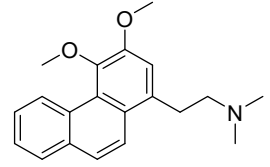
			<chem>C2=NOC3(C2)CC(=C(C(=CO3)Br)OC)Br)Br</chem>					
52	Psammalyisin H	C ₂₆ H ₃₀ Br ₄ F ₃ N ₃ O ₈	<chem>C[N+](C)(C)CC1=CC(=C(C(=C1)Br)OCCCN(C(=O)C2=NOC3(C2O)C=C(C(C(=CO3)Br)OC)Br)Br.C(=O)(C(F)(F)F)[O-]</chem>	against the P. falciparum strain 3D7		0.4 μM	Pseudoceratina sp.	(Tempone <i>et al.</i> , 2021).
53	psammalyisins G	C ₂₃ H ₂₆ Br ₄ N ₄ O ₇	<chem>CN(CCC1=CC(=C(C(=C1)Br)OCCCN(C(=O)C2=NOC3(C2O)C=C(C(C(=CO3)Br)OC)Br)Br)C(=O)N</chem>	against the P. falciparum strain 3D7		5.2 μM	Pseudoceratina sp.	(Tempone <i>et al.</i> , 2021).
54	Palauamine	C ₁₇ H ₂₂ ClN ₉ O ₂	<chem>C1C2C(C(C3(C2C45N1C(=O)C6=CC=CN6C4N=C(N5)N)C(N=C(N3)N)O)C1)CN</chem>	against T. b. rhodesiense and L. donovani		0.4 μg/mL 1.1 μg/mL	sponges of the Agelas and Axinella genera	(Tempone <i>et al.</i> , 2021).

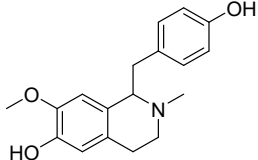
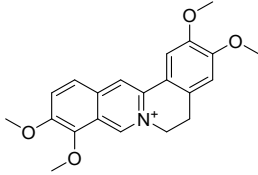
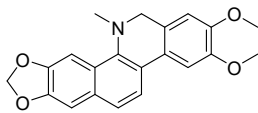
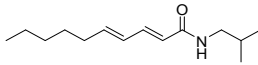
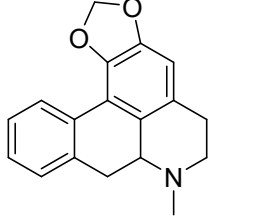
55	longamide B	C ₉ H ₈ Br ₂ N ₂ O ₃	C1C(N2C(=CC(=C2Br)Br)C(=O)N1)CC(=O)O	against T. b. rhodesiense and L. donovani		1.5 µg/mL 3.8 µg/mL	sponges of the Agelas and Axinella genera	(Tempone <i>et al.</i> , 2021).
56	dispacamide B	C ₁₁ H ₁₂ BrN ₅ O ₂	C1=C(NC=C1Br)C(=O)NCCC=C2C(=O)NC(=N2)N	against P. falciparum		1.3 µM	sponges of the Agelas and Axinella genera	(Tempone <i>et al.</i> , 2021).
57	spongiacidin B	C ₁₁ H ₁₂ BrN ₅ O ₂	C1CNC(=O)C2=C(C1=C3C(=O)NC(N3)N)C(=CN2)Br	against P. falciparum		1.1 µM	sponges of the Agelas and Axinella genera	(Tempone <i>et al.</i> , 2021).
58	Oroidin	C ₁₁ H ₁₁ Br ₂ N ₅ O	C1=C(NC(=C1Br)Br)C(=O)NCC=CC2=CN=C(N2)N	inhibition of the P. falciparum enoyl-ACP reductase (PfFabI) enzyme		0.77 µM	sponges of the Agelas and Axinella genera	(Tempone <i>et al.</i> , 2021).
59	Fascaplysin	C ₁₈ H ₁₁ ClN ₂ O	C1=CC=C2C(=C1)C3=C(N2)C4=[N+](C=C3)C5=CC=CC=C5N4	against T. b. rhodesiense		0.17 µg/mL	sponge Hyrtios cf. erecta	(Tempone <i>et al.</i> , 2021).

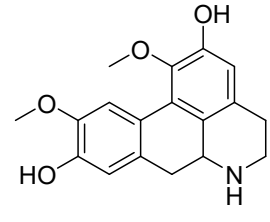
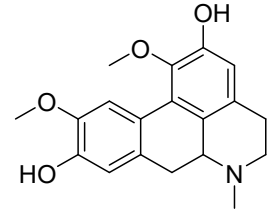
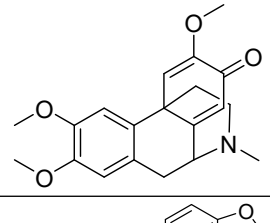
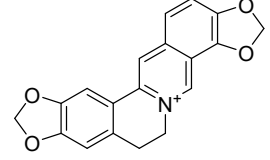
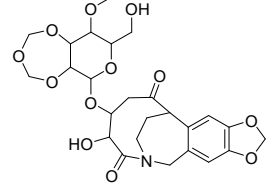
60	Staurosporine	C ₂₈ H ₂₆ N ₄ O ₃	5C4=O.[C1-] <chem>CC12C(C(CC(O1)N3C4=CC=CC=C4C5=C6C(=C7C8=CC=CC=C8N2C7=C53)CNC6=O)NC)OC</chem>	against L. major promastigotes, against T. b. brucei		5.3 μM 20 nM	sponge associated actinomycetes <i>Streptomyces</i> sp.	(Tempone <i>et al.</i> , 2021).
61	Tryptophol	C ₁₀ H ₁₁ NO	<chem>C1=CC=C2C(=C1)C(=CN2)CCO</chem>	against L. donovani amastigotes		9.6 μg/mL	<i>Spongia</i> sp., <i>Ircinia</i> sp.	(Tempone <i>et al.</i> , 2021).
62	Diazepinomicin	C ₂₈ H ₃₄ N ₂ O ₄	<chem>CC(=CCCC(=CCCC(=CCN1C2=C(C(=CC(=C2)O)O)NC3=C(C1=O)C=CC=C3O)C)C</chem>	against T. b. brucei trypomastigotes inhibit the T. b. brucei protease rhodesain		13.6 μM	<i>Micromonospora</i> sp.	(Tempone <i>et al.</i> , 2021).

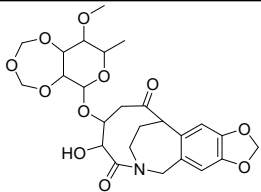
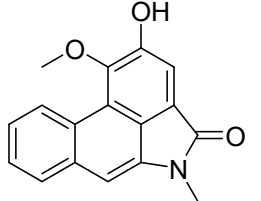
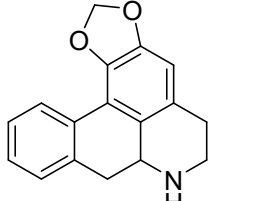
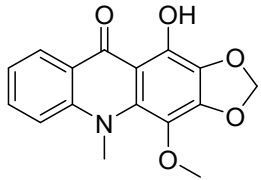
63	paenidigyamycin A	C36H52N4+2	<chem>CC1=C([N+](=C(N1CCCC2=CC=CC=C2)C3=[N+](C(=C(N3C)CC4=CC=CC=C4)C)CCC(C)C)CCC(C)C)C</chem>	Against (T. b. brucei trypomastigotes Against P. falciparum		0.78 μM 9.1 μM	mangrove rhizosphere soils	(Tempone <i>et al.</i> , 2021).
64	Ptilomycalin A	C45H83ClN6O5	<chem>CCC1CCCCC2(O1)CC3CCC4[N+]3=C(N2)NC5(C4C(=O)O)CCCCCCCCCCCCCCCC(=O)N(CCCCN)CCCN)CCCC(O5)C.[Cl-]</chem>	against P. falciparum		0.1 μM	sponge Monanchora arbuscula	(Tempone <i>et al.</i> , 2021).
65	2-n-propylquinoline	C12H13N	<chem>CCCC1=NC2=CC=CC=C2C=C1</chem>	against the promastigote forms of L. braziliensis and the epimastigote forms of T. cruzi		0.29 mM	Galipea longiflora K. Krause	(Osorio <i>et al.</i> , 2008).
66	Galipinine	C19H21NO2	<chem>CN1C(CCC2=C(C=CC=C2)CC)C3=CC4=C(C=C3)OCO4</chem>	Against chloroquine-resistant strains of P.		6.12 μM	Galipea officinalis Hancock	(Osorio <i>et al.</i> , 2008).

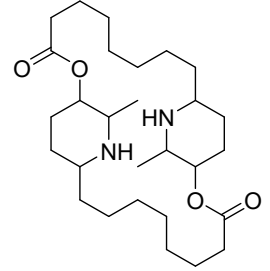
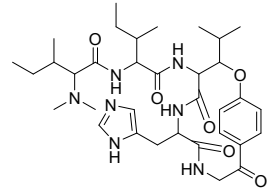
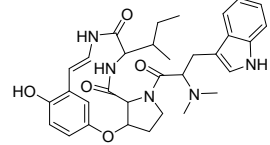
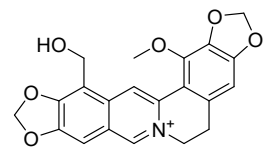
				falciparum				
67	Normelicopicine	C ₁₇ H ₁₇ N ₁ O ₅	<chem>CN1C2=CC=C(C=C2C(=O)C3=C1C(=C(C(=C3O)OC)OC)OC</chem>	against both chloroquine-sensitive (HB3) and chloroquine-resistant (K1) strains of <i>P. falciparum</i>		14.7 μM	Teclea trichocarpas	(Osorio <i>et al.</i> , 2008).
68	Quinine	C ₂₀ H ₂₄ N ₂ O ₂	<chem>COC1=CC2=C(C=CN=C2C=C1)C(C3CC4CCN3CC4C=C)O</chem>	Against <i>T. b. brucei</i>		4.9 μM	cinchona bark	(Osorio <i>et al.</i> , 2008).
69	Quinidine	C ₂₀ H ₂₄ N ₂ O ₂	<chem>COC1=CC2=C(C=CN=C2C=C1)C(C3CC4CCN3CC4C=C)O</chem>	Against <i>T. b. brucei</i>		0.8 μM	cinchona bark	(Osorio <i>et al.</i> , 2008).
70	Cinchonine	C ₁₉ H ₂₂ N ₂ O	<chem>C=CC1CN2CC1CC2C(C3=C(C=NC4=CC=C(C=C4)O</chem>	Against <i>T. b. brucei</i>		1.2 μM	cinchona bark	(Osorio <i>et al.</i> , 2008).

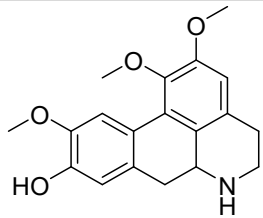
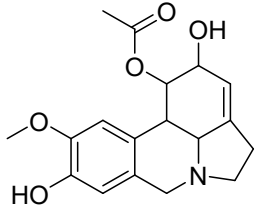
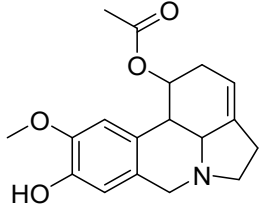
71	Crotsparine	C18H19NO3	<chem>CN1CCC2=CC(=C(C3=C2C1C34C=CC(=O)C=C4)O)OC</chem>	against the chloroquine-resistant FcB1 strain		7.41 μM	Uvaria klaineana	(Osorio <i>et al.</i> , 2008).
72	isoguattouregidine	C19H19NO5	<chem>CC1(C2=C(C=CC(=C2)O)C3=C(C(=C(C4=C3C1=NCC4)OC)O)OC)O</chem>	against the promastigote forms of L. donovani and L. amazonensis		0.29 mM	genus Guatteria	(Osorio <i>et al.</i> , 2008).
73	Liriodenine	C17H9NO3	<chem>C1OC2=C(O1)C3=C4C(=C2)C=CN=C4C(=O)C5=CC=CC=C53</chem>	Against P. falciparum		26.2 μM	Stephania dinklagei	(Osorio <i>et al.</i> , 2008).
74	Stephanine	C19H19NO3	<chem>CN1CCC2=CC3=C(C4=C2C1CC5=C4C=CC=C5OC)OCO3</chem>	against the T9/94 strain of P. falciparum		0.38 μM	Stephania venosa	(Osorio <i>et al.</i> , 2008).
75	Atherosperminine	C20H23NO2	<chem>CN(C)CCC1=C(C(=C(C2=C1C=CC3=CC=CC=C32)OC)OC</chem>	against a chloroquine-resistant strain of P. falciparum		5.80 μM	stem bark of Cryptocarya nigra	(Uzor, 2020b).

76	(+)-N-methylisococlaurine	C ₁₈ H ₂₁ NO ₃	<chem>CN1CCC2=CC(=C(C=C2C1CC3=CC=C(C=C3)O)OC)O</chem>	(K1 strain) against a chloroquine-resistant strain of <i>P. falciparum</i> (K1 strain)		5.40 μM	stem bark of <i>Cryptocarya nigra</i>	(Uzor, 2020b).
77	Palmatine	C ₂₁ H ₂₂ NO ₄ ⁺	<chem>COC1=C(C2=C[N+]3=C(C=C2C=C1)C4=CC(=C(C=C4CC3)OC)OC)OC</chem>	against <i>P. falciparum</i> K1 strain		0.080 μg/mL	leaves of <i>Annickia kummeriae</i>	(Uzor, 2020b).
78	Dihydroneitidine	C ₂₁ H ₁₉ NO ₄	<chem>CN1CC2=CC(=C(C=C2C3=C1C4=CC5=C(C=C4C=C3)OCO5)OC)OC</chem>	antiparasitic activity		25 nM	<i>Zanthoxylum heitzii</i> (Rutaceae) bark	(Uzor, 2020b).
79	Pellitorine	C ₁₄ H ₂₅ NO	<chem>CCCCC=CC=CC(=O)NCC(C)C</chem>	antiparasitic activity		9.7 μM	<i>Zanthoxylum heitzii</i> (Rutaceae) bark	(Uzor, 2020b).
80	Roemerine	C ₁₈ H ₁₇ NO ₂	<chem>CN1CCC2=CC3=C(C4=C2C1CC5=CC=CC=C54)OCO3</chem>	inhibitory activity against the growth of <i>P. falciparum</i> 3D7 clone		1.49 μg/mL	leaves of <i>Phoebe tavoyana</i> (Meissn.) Hook f. (Lauraceae)	(Uzor, 2020b).

81	Lauro litsine	C ₁₈ H ₁₉ NO ₄	<chem>COC1=C(C=C2CC3C4=C(C2=C1)C(=C(C=C4CCN3)O)OC)O</chem>	inhibitory activity against the growth of <i>P. falciparum</i> 3D7 clone		1.65 µg/mL	leaves of <i>Phoebe tavoyana</i> (Meissn.) Hook f. (Lauraceae)	(Uzor, 2020b).
82	boldine	C ₁₉ H ₂₁ NO ₄	<chem>CN1CCC2=CC(=C(C3=C2C1C4=CC(=C(C=C43)OC)O)OC)O</chem>	inhibitory activity against the growth of <i>P. falciparum</i> 3D7 clone		2.76 µg/ml	leaves of <i>Phoebe tavoyana</i> (Meissn.) Hook f. (Lauraceae)	(Uzor, 2020b).a
83	Sebiferine	C ₂₀ H ₂₃ NO ₄	<chem>CN1CCC23C=C(C(=O)C=C2C1CC4=CC(=C(C=C34)OC)O)C)OC</chem>	against <i>P. falciparum</i> KI strain		22.46 µM	<i>Dehaasia longipedicellata</i>	(Uzor, 2020b).
84	Coptisine	C ₁₉ H ₁₄ NO ₄ ⁺	<chem>C1C[N+]2=C(C=C3C=CC4=C(C3=C2)OCO4)C5=CC6=C(C=C5)OCO6</chem>	inhibitor of <i>Plasmodium falciparum</i> dihydroorotate dehydrogenase		1.83 µM	<i>Coptidis rhizoma</i>	(Uzor, 2020b).
85	cripowellin A	C ₂₅ H ₃₁ NO ₁₂	<chem>COC1C(OC(C2C1OCOCO2)OC3CC(=O)C4CN(CC5=CC6=C(C=C5)OCO6)C(=C45)OCO</chem>	antiplasmodial activity		30 nM	swamp lily <i>Crinum erubescens</i>	(Uzor, 2020b).

			6)C(=O)C3O)C O					
86	Cripowellin C	C25H31NO11	CC1C(C2C(C(O1)OC3CC(=O)C4CCN(CC5=CC6=C(C=C45)OCO6)C(=O)C3O)OCOCO2)O C	antiplasmodial activity		26 nM	swamp lily <i>Crinum erubescens</i>	(Uzor, 2020b).
87	Sauristolactam	C17H13NO3	CN1C2=CC3=CC=CC=C3C4=C2C(=CC(=C4)OC)O)C1=O	Against a chloroquine-sensitive <i>P.falciparum</i> line(3D7)		9.0 μM	aerial parts of <i>Goniolium australe</i>	(Uzor, 2020b).
88	(-)-anonaine	C17H15NO2	C1CNC2CC3=CC=CC=C3C4=C2C1=CC5=C4OCOC5	Against a chloroquine-sensitive <i>P.falciparum</i> line 3D7		7.0 μM	aerial parts of <i>Goniolium australe</i>	(Uzor, 2020b).
89	Normelicopidine	C16H13NO5	CN1C2=CC=C(C=C2C(=O)C3=C1C(=C4C(=C3O)OCO4)OC	parasite <i>P. falciparum</i> Dd ₂		18.9 ug/mL	root bark of <i>Zanthoxylum simullans</i>	(Uzor, 2020b).

90	Carpaine	C28H50N2O4	<chem>CC1C2CCC(N1)CCCCCCC(=O)OC3CCC(CC(C)CCCC(=O)O2)NC3C</chem>	strains of <i>P. falciparum</i> 3D7		4.21 μM	<i>Carica papaya</i> L	(Uzor, 2020b).
91	hymenocardine-H	C34H51N7O6	<chem>CCC(C)C(C(=O)NC1C(OC2=C(C=C(C=C2)C(=O)CNC(=O)C(NC1=O)CC3=CN=CN3)C(C)C)NC(=O)C(C)CC)N(C)C</chem>	antiplasmodial activity		27.9 μM	root bark of <i>Hymenocardia</i>	(Uzor, 2020b).
92	O-desmethylnummularine-R	C32H39N5O5	<chem>CCC(C)C1C(=O)NC=CC2=C(C=CC(=C2)OC3CCN(C3C(=O)N1)C(=O)C(C4=CNC5=CC=CC=C54)N(C)C)O</chem>	antiplasmodial activity against <i>P. falciparum</i> K1		3.2 μM	Roots of <i>Ziziphus oxyphylla</i>	(Uzor, 2020b).
93	simplicifolianine	C21H18NO6+	<chem>COC1=C2C(=CC3=C1OC(=O)C[N+]4=CC5=CC6=C(C(=C5)C=C24)CO)OC(=O)O6</chem>	antiplasmodial activity against the <i>P. falciparum</i> strains, TM4/8.2		0.78 $\mu\text{g/mL}$ 1.29 $\mu\text{g/mL}$	aerial parts of <i>Meconopsis simplicifolia</i> (D. Don) Walpers (Papaveraceae)	(Uzor, 2020b).

				(chloroquine-antifolate-sensitive strain) and K1CB1 (multidrug-resistant strain)				
94	(+)-laurotetanine	C19H21NO4	<chem>COC1=C(C2=C3C(CC4=CC(=C(C=C42)OC)O)NCCC3=C1)OC</chem>	Antiplasmodial activity		0.189 μ M	<i>Alseodaphne corneri</i> .	(Uzor, 2020b).
95	Sternbergine	C18H21NO5	<chem>CC(=O)OC1C(C=C2CCN3C2C1C4=CC(=C(C=C4C3)O)OC)O</chem>	Against <i>P. falciparum</i> strain D10		3.9 μ g/mL	<i>B. radulosa</i>	(Nair and van Staden, 2019).
96	1-O-Acetylnorpluviine	C18H21NO4	<chem>CC(=O)OC1CC=C2CCN3C2C1C4=CC(=C(C=C4C3)O)OC</chem>	Against <i>P. falciparum</i> strain D10		28.3 μ g/mL	<i>B. radulosa</i>	(Nair and van Staden, 2019).

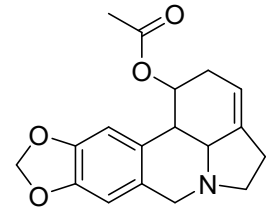
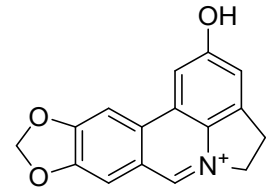
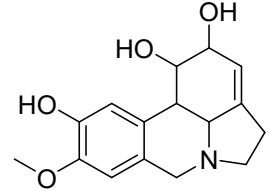
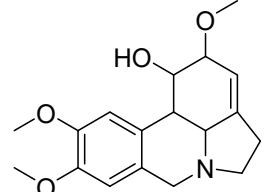

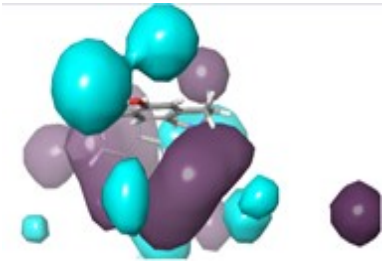



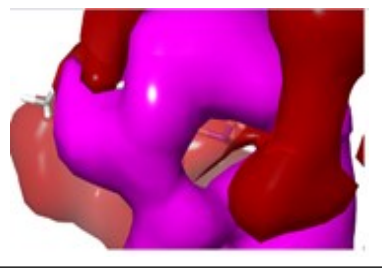
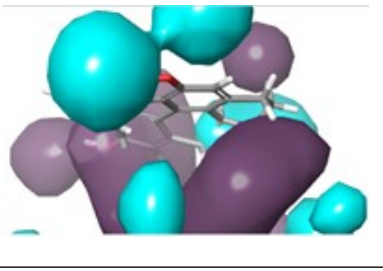


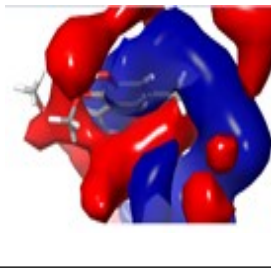
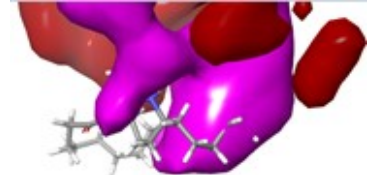
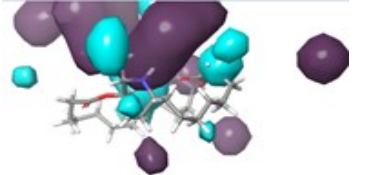
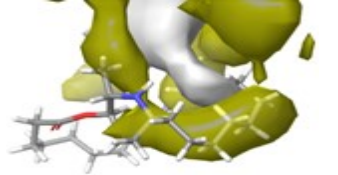
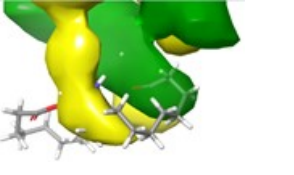
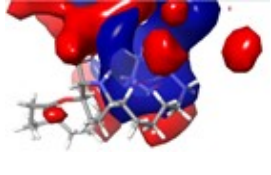
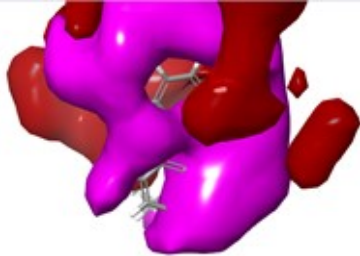
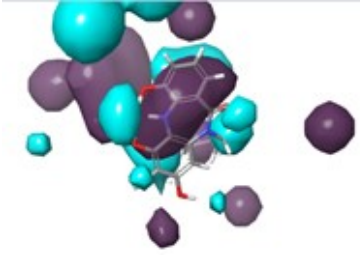
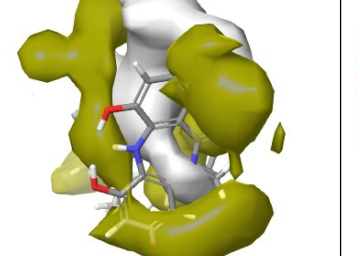
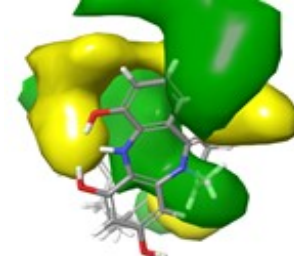
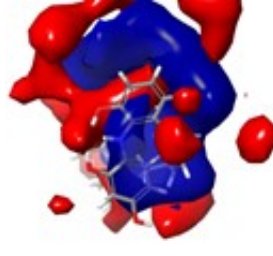
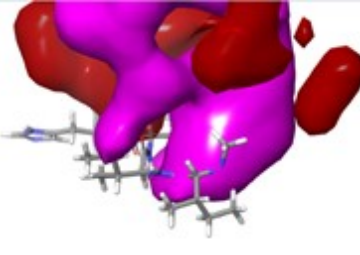
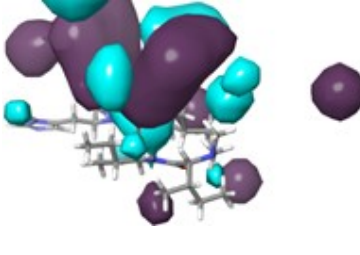

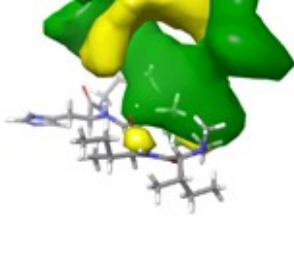
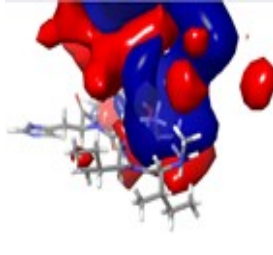
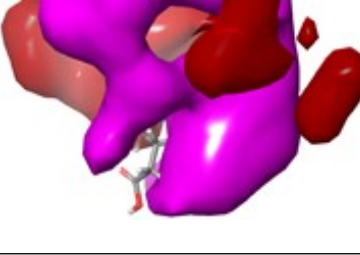
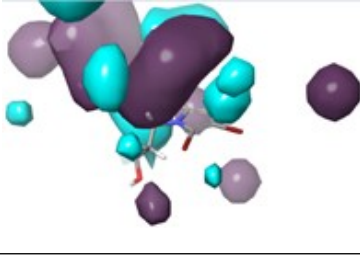
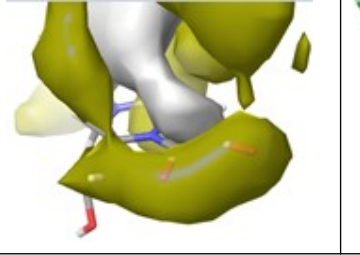
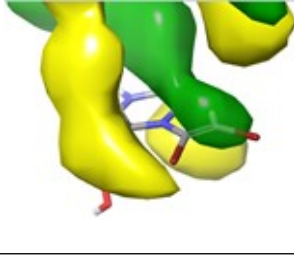

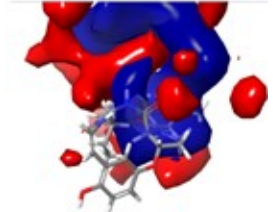
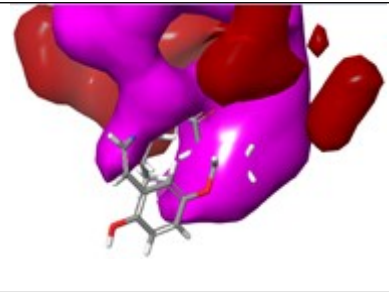
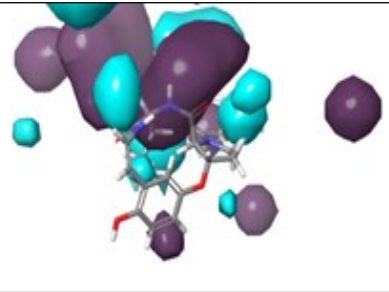
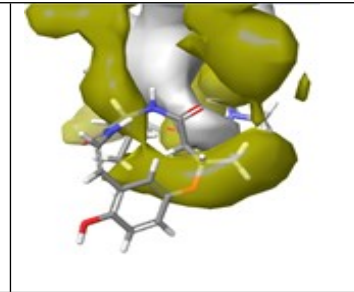
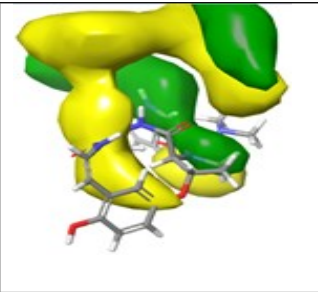

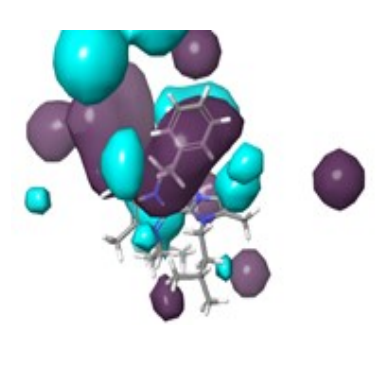
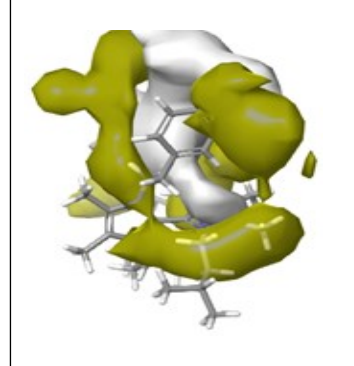
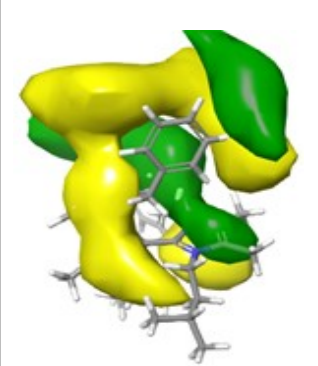
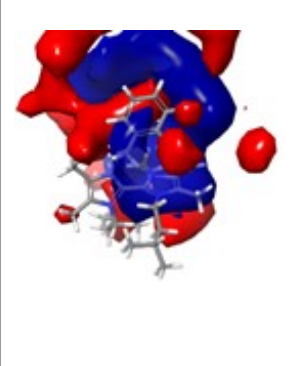
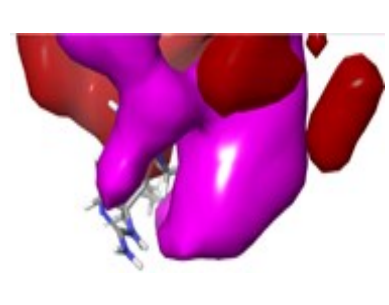
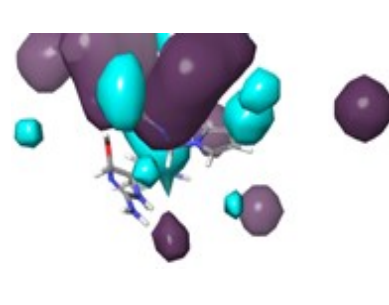
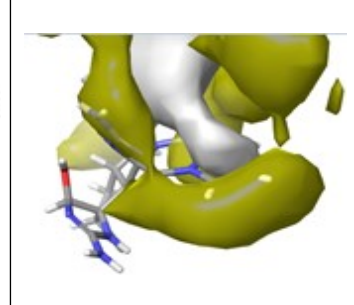
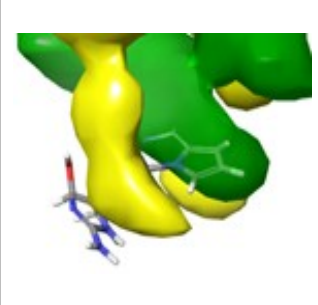
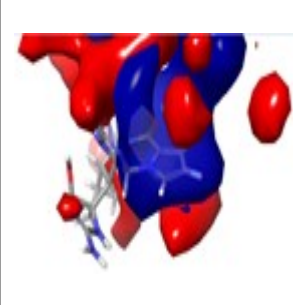
97	Acetylcaranine	C ₁₈ H ₁₉ NO ₄	<chem>CC(=O)OC1CC=C2CCN3C2C1C4=CC5=C(C=C4C3)OCO5</chem>	Against P. falciparum strain Dd2		1.1 µg/mL	A. belladonna	(Nair and van Staden, 2019).
98	Ungeremine	C ₁₆ H ₁₂ NO ₃ ⁺	<chem>C1C[N+]2=CC3=CC4=C(C=C3C5=CC(=CC1=C52)O)OCO4</chem>	Against P. falciparum strain K1		0.088 µg/mL	Phaedranassa dubia	(Nair and van Staden, 2019).
99	Pseudolycorine	C ₁₆ H ₁₉ NO ₄	<chem>COC1=C(C=C2C3C(C(C=C4C3N(CC4)CC2=C1)O)O)O</chem>	Against P. falciparum strain K1		0.24 µg/mL	P. dubia	(Nair and van Staden, 2019).
100	Galanthine	C ₁₈ H ₂₃ NO ₄	<chem>COC1C=C2CCN3C2C(C1O)C4=CC(=C(C=C4C3)OC)OC</chem>	Against P. falciparum strain K1		0.2 µg/mL	Z. citrina	(Nair and van Staden, 2019).

Table S-2: Visualization of Contour Maps from the Field-Based QSAR Study.

Compound	Gaussian	Gaussian	Gaussian	Gaussian	Gaussian
----------	----------	----------	----------	----------	----------

	H-bond acceptor	H-bond donor	Hydrophobic	Steric	Electrostatic
(+)-N-methylisococlaurine					
Boldine					
Carpaine					

diazepinomicin					
hymenocardine-H					
longamide B					
O-desmethylnumarine-R					

					
paenidigyamin A					
Palauamine					
spongiacidin B					

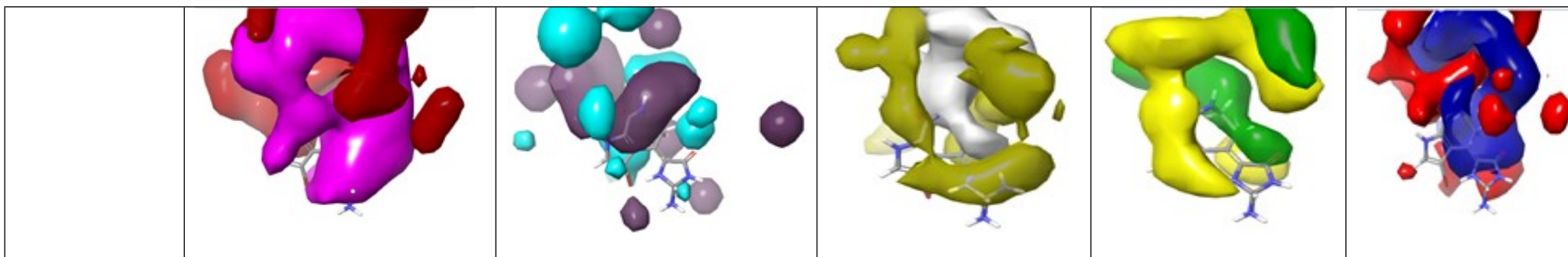
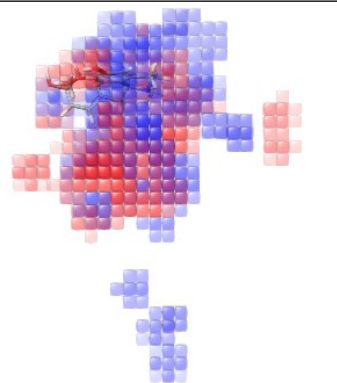
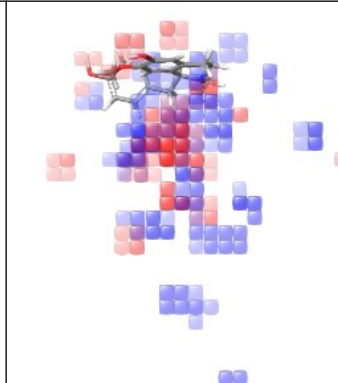
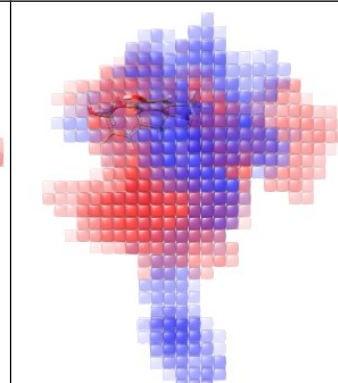
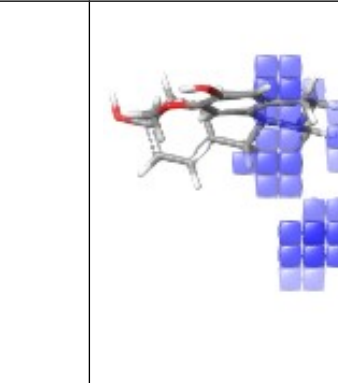
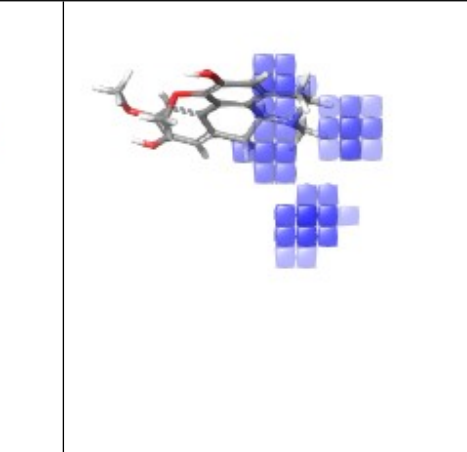
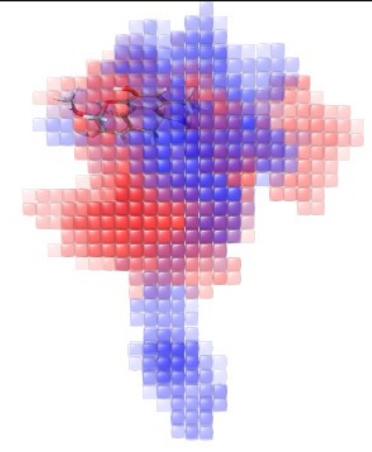
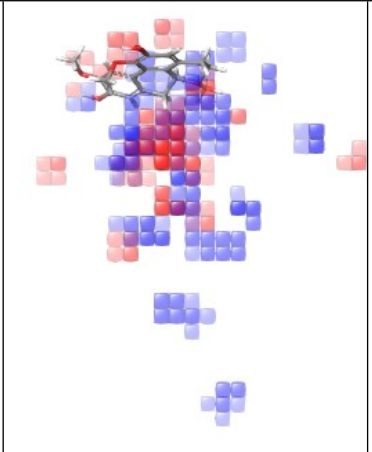
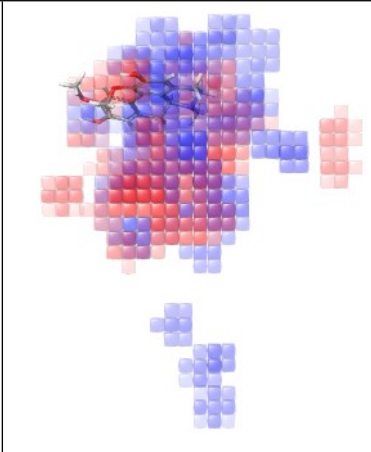


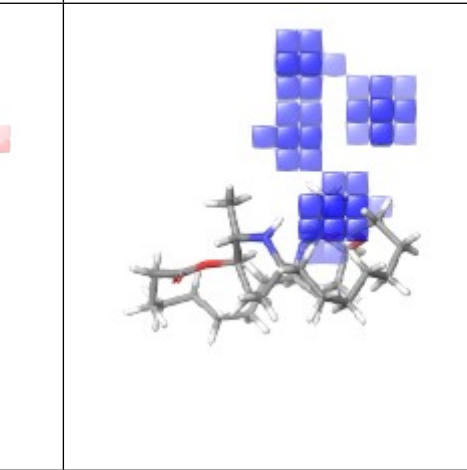
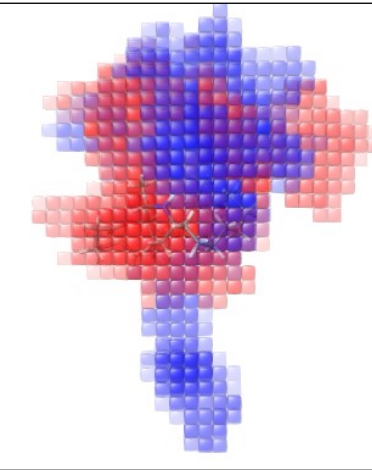
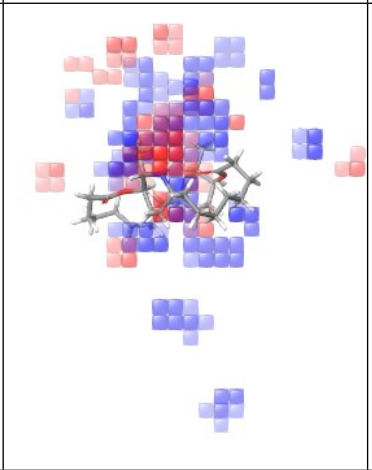
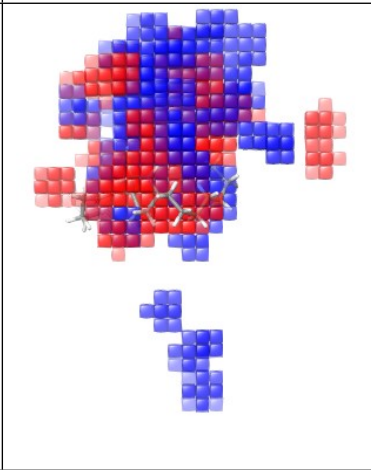
Table S-3: Atom-Based QSAR Contour Map Visualization

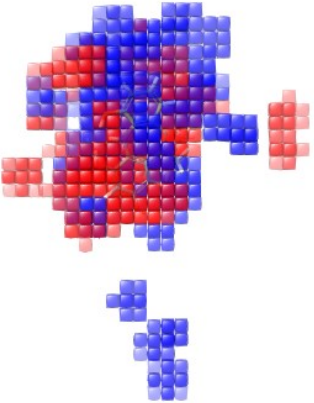
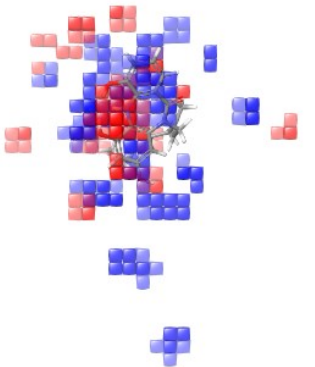
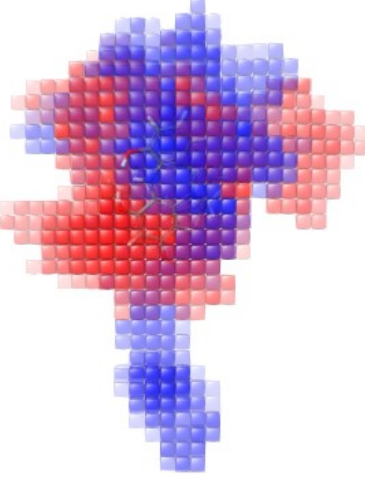

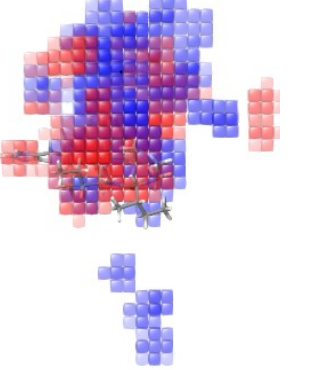
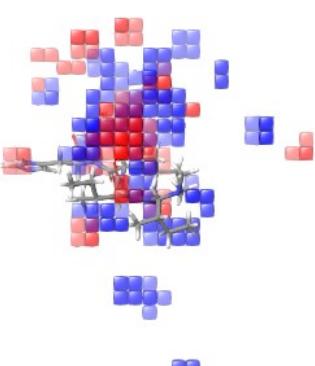
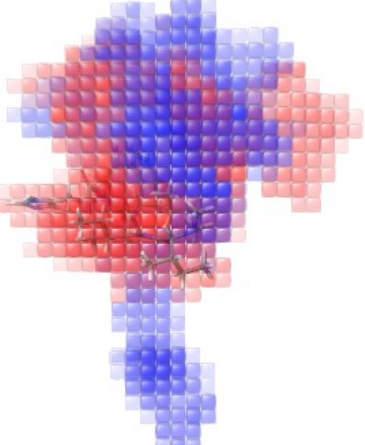
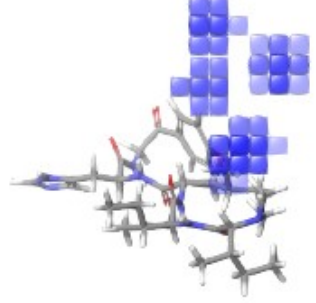
Compound	Electron withdrawing	H-bond donor	Hydrophobic	Positive ionic
(+)-N-methylisococlaurine				

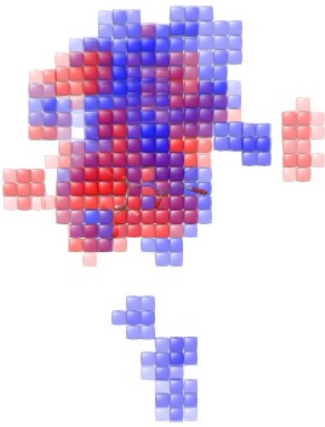
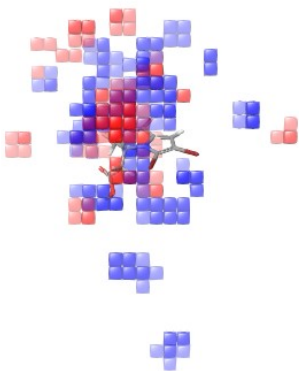
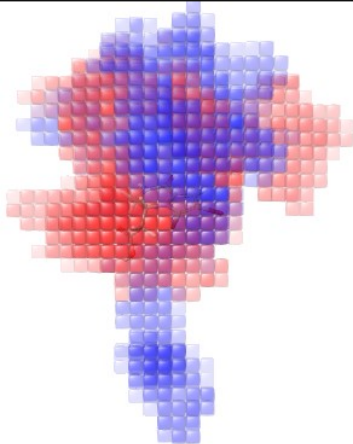

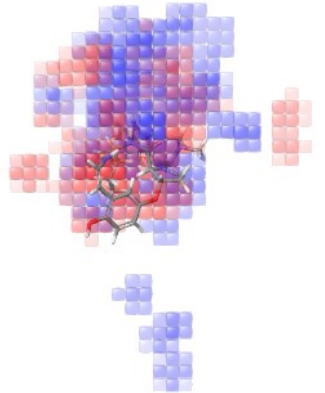
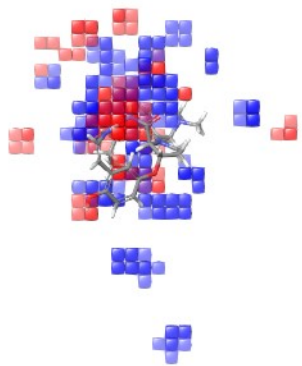
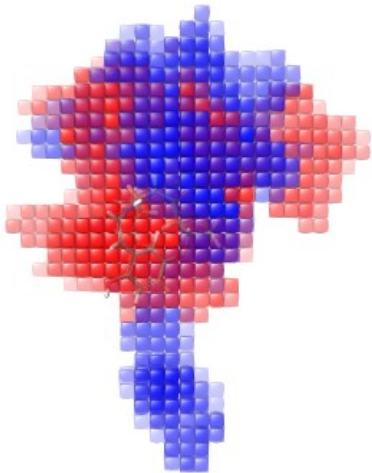

Boldine

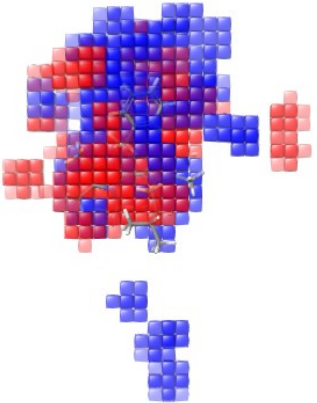
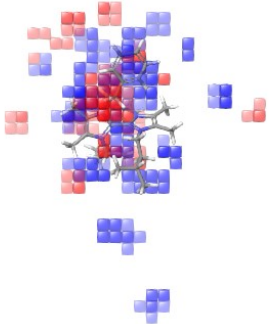
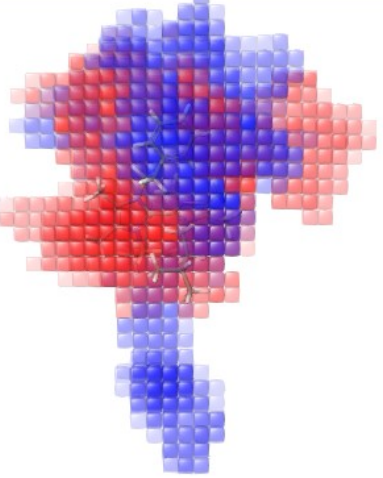
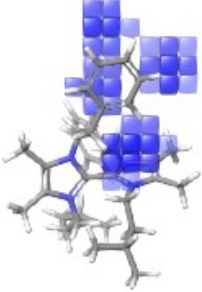
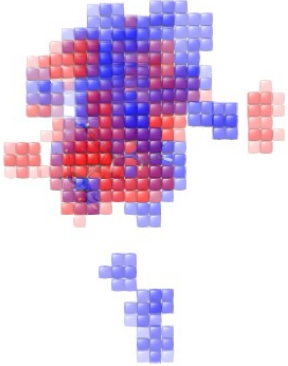
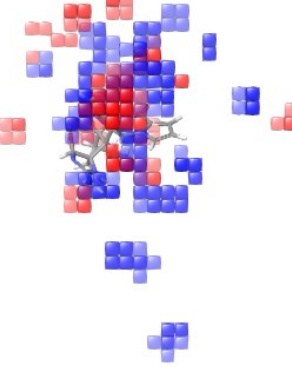
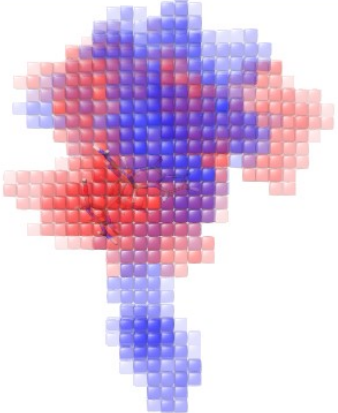



Carpaine



Diazepinomicin	 A top-down electrostatic potential map of Diazepinomicin. The molecule is represented by a grid of red and blue squares. The red squares, indicating negative charge, are concentrated in the lower-left and central regions. The blue squares, indicating positive charge, are primarily in the upper-right and central regions.	 A side-view electrostatic potential map of Diazepinomicin. The molecule is shown as a grey stick model with a semi-transparent electrostatic potential surface. The surface is colored red where it is negatively charged and blue where it is positively charged.	 A back-view electrostatic potential map of Diazepinomicin. The molecule is shown as a grey stick model with a semi-transparent electrostatic potential surface. The surface is colored red where it is negatively charged and blue where it is positively charged.	 A front-view electrostatic potential map of Diazepinomicin. The molecule is shown as a grey stick model with a semi-transparent electrostatic potential surface. The surface is colored red where it is negatively charged and blue where it is positively charged.
hymenocardine-H	 A top-down electrostatic potential map of hymenocardine-H. The molecule is represented by a grid of red and blue squares. The red squares, indicating negative charge, are concentrated in the lower-left and central regions. The blue squares, indicating positive charge, are primarily in the upper-right and central regions.	 A side-view electrostatic potential map of hymenocardine-H. The molecule is shown as a grey stick model with a semi-transparent electrostatic potential surface. The surface is colored red where it is negatively charged and blue where it is positively charged.	 A back-view electrostatic potential map of hymenocardine-H. The molecule is shown as a grey stick model with a semi-transparent electrostatic potential surface. The surface is colored red where it is negatively charged and blue where it is positively charged.	 A front-view electrostatic potential map of hymenocardine-H. The molecule is shown as a grey stick model with a semi-transparent electrostatic potential surface. The surface is colored red where it is negatively charged and blue where it is positively charged.

<p>longamide B</p>				
<p>O-desmethylnummularine-R</p>				

paenidigyamycin A	 A 3D electrostatic potential map of paenidigyamycin A, showing a complex, multi-lobed structure. The map is color-coded by charge, with red indicating negative charge and blue indicating positive charge. The molecule is shown in a perspective view, highlighting its overall shape and charge distribution.	 A 3D electrostatic potential map of paenidigyamycin A, similar to the first image, but with a stick model of the molecule overlaid. The stick model is rendered in a grey and red color scheme, showing the carbon and oxygen atoms respectively. This view allows for a direct comparison between the electrostatic potential and the molecular structure.	 A 3D electrostatic potential map of paenidigyamycin A, showing a different perspective or a different set of parameters compared to the first image. The red and blue regions are more pronounced, indicating a different charge distribution.	 A 3D electrostatic potential map of paenidigyamycin A with a stick model overlaid. The stick model is rendered in a grey and blue color scheme, showing the carbon and nitrogen atoms respectively. This view highlights the interaction between the electrostatic potential and the nitrogen-containing functional groups.
Palauamine	 A 3D electrostatic potential map of Palauamine, showing a complex, multi-lobed structure. The map is color-coded by charge, with red indicating negative charge and blue indicating positive charge. The molecule is shown in a perspective view, highlighting its overall shape and charge distribution.	 A 3D electrostatic potential map of Palauamine, similar to the first image, but with a stick model of the molecule overlaid. The stick model is rendered in a grey and red color scheme, showing the carbon and oxygen atoms respectively. This view allows for a direct comparison between the electrostatic potential and the molecular structure.	 A 3D electrostatic potential map of Palauamine, showing a different perspective or a different set of parameters compared to the first image. The red and blue regions are more pronounced, indicating a different charge distribution.	 A 3D electrostatic potential map of Palauamine with a stick model overlaid. The stick model is rendered in a grey and blue color scheme, showing the carbon and nitrogen atoms respectively. This view highlights the interaction between the electrostatic potential and the nitrogen-containing functional groups.

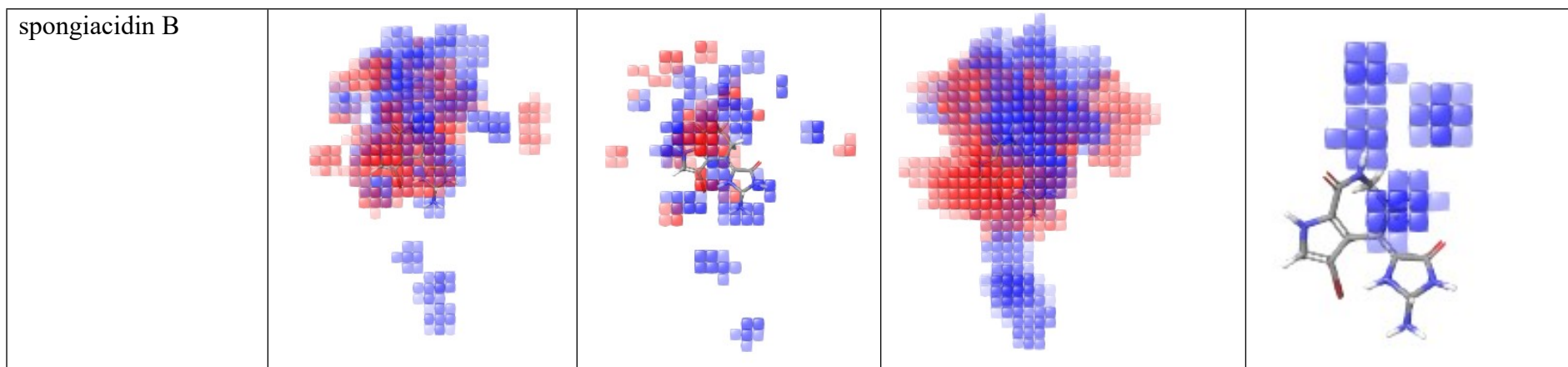


Table S-4: Ramachandran Plot Statistics

Ramachandran Plot	PDB ID											
	7AVT	6SFR	6YNE	6W8H	7JX2	7JWR	7JVY	7JZ5	7JWD	6W81	6VF1	6UX9
Residues in most favored regions	778=93.8%	770=93.0%	1049=91.1%	335=93.1%	112=90.3%	232=92.4%	228=91.9%	229=92.3%	230=92.0%	479=92.1%	267=94.3%	519=92.0%
Residues in Additional Allowed regions	51= 6.2%	58=7.0%	95=8.2%	23=6.4%	11=8.9%	17=6.8%	18=7.3%	17=6.9%	18=7.2%	38=7.3%	16=5.7%	43=7.6%
Residues in generously allowed regions	0=0.0%	0=0.0%	4=0.3%	2=0.6%	1=0.8%	2=0.8%	2=0.8%	2=0.8%	2=0.8%	1=0.2%	0=0.0%	2=0.4%
Residues in disallowed regions	0=0.0%	0=0.0%	4=0.3%	0=0.0%	0=0.0%	0=0.0%	0=0.0%	0=0.0%	0=0.0%	2=0.4%	0=0.0%	0=0.0%

Number of non-glycine and non-proline residues	829=100.0%	828=100.0%	1152=100.0%	360=100.0%	124=100.0%	251=100.0%	248=100.0%	248=100.0%	250=100.0%	520=100.0%	283=100.0%	564=100.0%
Number of end-residues	7	7	4	3	2	4	3	3	4	4	22	13
Number of glycine residues	29	29	132	14	9	18	18	18	18	66	26	24
Number of proline residues	64	64	48	20	0	1	1	1	1	12	18	27
Total number of residues	929	928	1336	397	135	274	270	270	273	602	349	628

Table S-5: Docking score and interactions of compounds with their respective proteins

Protein	Compounds name	No. of interactions	Residues	Types of protein-ligand interaction by	Distance	Docking score	H-bond
6UX9	(+)N-methylisococlaurine	1	ASP 359	H-bonding	2.14	-7.727	1
		1	PHE 134	Pi-pi stacking	4.29		
	spongiacidin B	1	ASN 198	H-Bonding	1.92	-6.736	2
		1	ASN 124	H-bonding	1.85		
	Diazepinomicin	1	LYS 228	Pi-cation	4.46	-6.431	3
		1	ASP 211	H-bonding	1.71		
		1	LYS 234	H-bonding	2.35		
		1	GLU 225	H-bonding	1.72		
	Boldine	1	ASN 198	H-bonding	2.02	-5.972	1
	longamide B	1	VAL 199	Halogen bond	2.46	-5.279	1
		1	PHE 200	Pi-pi stacking			
		1	LYS 209	H-bonding	1.84		
Palauamine	1	ASP 359	H-bonding	2.13	-4.455	3	
	1	ALA 132	H-bonding	1.95			
	1	GLU 225	H-bonding	1.65			

	Oseltamivir	1	VAL-199	H-bonding	1.69	-7.119	3
		1	ASP-359	H-bonding	2.47		
		1	LYS—145	H-bonding	2.68		
<i>6VFI</i>	(+)–N-methylisococlaurine	1	GOA 506	H-bonding	1.58	-8.672	1
		2	MG 502	Metal-coordination	2.10		
			MG 502	Metal-coordination	2.38		
	Palauamine	1	ASP 418	H-bonding	2.46	-8.258	1
		1	MG 502	Metal coordination	2.06		
		1	MG 501	Metal coordination	2.22		
	longamide B	1	GOA 506	H-bonding	2.00	-7.86	1
		2	MG 502	Metal coordination	1.99		
			MG 502	Metal coordination	2.36		
		1	MG 501	Metal coordination	2.25		
	Boldine	1	MG 502	Metal coordination	2.24	-7.588	0
		1	MG 501	Metal coordination	2.07		
spongiacidin B	1	GOA 506	H-bonding	2.50	-7.087	1	
	1	MG 502	Metal coordination	2.06			
	1	MG 501	Metal coordination	2.27			
Diazepinomicin	1	MG 501	Metal coordination	2.28	-6.499	0	
	1	TRP 434	Pi-pi stacking	3.96			
Carpaine	1	MG 502	Metal coordination	2.13	-6.238	0	
hymenocardine-H	1	MG 501	Metal coordination	2.42	-5.898	0	
	1	MG 502	Metal coordination	2.04			
Oseltamivir	1	GOA 506	H-bonding	1.79	-7.833	2	
	1	GLY 433	H-bonding	1.89			
	1	MG 501	Metal coordination	2.27			
	1	MG 502	Metal coordination	2.06			
<i>6W81</i>	hymenocardine-H	2	GLU 165	H-bonding	2.29	-7.635	3
			GLU 165	H-bonding	1.60		
		1	HIE 162	H-bonding	1.91		
	(+)–N-methylisococlaurine	1	GLN 191	H-bonding	1.90	-7.043	1
	Palauamine	1	PRO 188	H-bonding	2.73	-6.988	4
2		GLN 191	H-bonding	1.96			
		GLN 191	H-bonding	2.05			
1		GLU 165	H-bonding	2.12			
Boldine	1	GLU 165	H-bonding	1.81	-6.764	1	

	spongiacidin B	1	HIE 162	H-bonding	1.99	-6.698	3
		1	ILE 140	H-bonding	1.93		
		1	GLY 142	H-bonding	2.14		
	Diazepinomicin	1	GLU 165	H-bonding	2.52	-6.332	2
		1	THR 189	H-bonding	1.81		
	paenidigyamycin A	1	HIE 41	Pi-pi stacking	5.36	-5.766	0
	longamide B	1	GLU 165	Halogen bond	3.22	-5.543	0
	O-desmethylnummularine-R	1	GLU 165	H-bonding	2.71	-5.355	3
1		ALA 143	H-bonding	2.68			
1		GLY 142	H-bonding	2.36			
Carpaine	1	GLY 142	H-bonding	2.33	-5.053	1	
Oseltamivir	1	GLN 187	H-bonding	1.99	-5.131	2	
	1	GLY 167	H-bonding	2.51			
7JWD	Diazepinomicin	1	GLU 72	H-bonding	1.69	-8.068	2
		1	ASP 78	H-bonding	2.43		
		1	TYR 19	Pi-pi stacking	5.03		
	Boldine	1	ASP 78	H-bonding	2.13	-7.823	1
		1	PHE 16	Pi-pi stacking	5.01		
	(+)-N-methylisococlaurine	1	PHE 16	Pi-pi stacking	5.35	-7.512	0
	spongiacidin B	-	-	-	-	-7.262	0
longamide B	1	THR 53	H-bonding	2.04	-6.897	1	
	1	PHE 16	Pi-pi stacking	5.15			
Oseltamivir	-	-	-	-	-5.591	0	
7JZ5	Boldine	1	TYR 19	H-bonding	1.98	-9	1
	Diazepinomicin	1	THR 51	H-bonding	2.51	-8.623	2
		1	ARG 104	H-bonding	2.25		
		1	TYR 60	Pi-pi stacking	5.20		
		1	TYR 19	Pi-pi stacking	5.18		
	(+)N-methylisococlaurine	1	LYS 40	H-bonding	2.37	-7.467	1
		1	PHE 16	Pi-pi stacking	5.11		
spongiacidin B	-	-	-	-	-7.252	0	
longamide B	1	GLN 38	Halogen bond	2.76	-6.936	4	
	1	GLN 108	H-bonding	2.06			
	1	GLN 97	H-bonding	1.79			
	1	LYS 40	H-bonding	1.95			
	1	GLU 72	H-bonding	2.58			

	Oseltamivir	1	LYS 40	H-bonding	2.02	-6.632	2
		1	ARG 104	H-bonding	2.39		
7JYV	Diazepinomicin	1	ASP 78	H-bonding	1.80	-8.351	1
	Boldine	1	PHE 16	Pi-pi stacking	5.45	-8.117	0
	(+)-N-methylisococlaurine	1	PHE 16	Pi-pi stacking	5.49	-7.982	0
	spongiacidin B	-	-	-	-	-7.081	0
	longamide B	1	GLN 97	H-bonding	1.94	-7.08	4
		1	GLU 72	H-bonding	2.27		
		1	GLN 108	H-bonding	2.42		
		1	LYS 40	H-bonding	1.83		
	1	LYS 40	Halogen bond	2.69			
	1	GLN 38	Halogen bond	2.87			
	Oseltamivir	1	GLN 38	H-bonding	2.63	-6.355	1
7JWR	Diazepinomicin	-	-	-	-	-9.417	0
	Boldine	1	TYR 19	H-bonding	2.13	-9.152	1
	(+)-N-methylisococlaurine	1	TYR 19	H-bonding	2.15	-8.091	1
	spongiacidin B	1	TYR 19	H-bonding	2.10	-7.317	1
	longamide B	1	THR 53	H-bonding	1.88	-6.932	1
		1	PHE 16	Pi-pi stacking	5.32		
		Oseltamivir	-	-	-	-	-6.329
7jx2	(+)-N-methylisococlaurine	1	TYR 19	H-bonding	2.68	-7.607	1
	Diazepinomicin	1	THR 53	H-bonding	2.20	-7.384	1
		1	PHE 16	Pi-pi stacking	5.14		
	longamide B	1	GLN 108	H-bonding	2.14	-7.217	4
		1	LYS 40	H-bonding	2.00		
		1	GLU 72	H-bonding	2.49		
		1	GLN 97	H-bonding	1.78		
		1	LYS 40	Halogen bond	2.48		
		1	GLN 38	Halogen bond	3.11		
	spongiacidin B	1	GLN 38	H-bonding	2.26	-6.953	1
	1	PHE 16	Pi-pi stacking	5.08			
Boldine	1	PHE 16	Pi-pi stacking	4.73	-6.824	0	
Oseltamivir	1	ARG 58	H-bonding	2.41	-6.674	2	
	1	THR 53	H-bonding	1.90			

6W8H	Diazepinomicin	3	GSH 201	H-bonding	1.88	-7.948	3
			GSH 201	H-bonding	1.90		
			GSH 201	H-bonding	1.67		
	Boldine	1	GSH 201	H-bonding	1.97	-7.192	1
	(+) -N-methylisococlaurine	2	TRP 104	Pi-pi stacking	4.30	-6.339	0
			TRP 104	Pi-pi stacking	4.33		
	Palauamine 2	1	TRP 104	H-bonding	1.80	-5.485	1
		1	GLN 36	Halogen bond	2.20		
	spongiacidin B	1	ARG 14	Halogen bond	2.72	-5.482	0
paenidigyamycin A	2	TRP 104	Pi-pi stacking	3.73	-4.785	0	
		TRP 104	Pi-pi stacking	3.93			
	1	PHE 16	Pi-pi stacking	5.17			
longamide B	2	LYS 112	Pi-cation	3.44			
		LYS 112	Pi-cation	6.45			
	-	-	-	-			-4.341
Oseltamivir	1	GLN 36	H-bonding	2.02	-4.229	1	
6YNE	Diazepinomicin	1	ASN 136	H-bonding	2.15	-5.664	1
		1	PHE 131	Pi-pi stacking	5.03		
	Palauamine	1	LYS 219	H-bonding	2.15	-4.958	2
		1	MET 130	H-bonding	2.03		
	(+) -N-methylisococlaurine	1	SER 125	H-bonding	2.20	-4.921	1
	spongiacidin B	1	ASN 136	H-bonding	2.08	-4.913	2
		1	LYS 139	H-bonding	2.66		
	Boldine	1	ASN 136	H-bonding	2.32	-4.781	3
		1	LYS 219	H-bonding	2.19		
		1	ASP 127	H-bonding	1.79		
longamide B	1	LYS 219	H-bonding	1.60	-4.521	3	
	1	LYS 139	H-bonding	2.61			
	1	LYS 139	H-bonding	2.58			
Oseltamivir	1	ASN 136	H-bonding	2.30	-3.941	1	
6SFR	(+) -N-methylisococlaurine	1	GLU 909	H-bonding	1.66	-6.181	1
	spongiacidin B	1	TYR 884	Pi-pi stacking	4.93	-5.906	1
		1	ASN 879	H-bonding	1.94		
	Boldine	1	ASN 879	H-bonding	1.79	-5.767	1
1		TYR 884	Pi-pi stacking	5.36			
	1	IMD 1102	Pi-pi stacking	5.08			

	longamide B	1	LEU 901	H-bonding	1.70	-5.616	1
		1	IMD 1102	Pi-pi stacking	5.30		
	O-desmethylnummularine-R	1	TYR 884	Pi-pi stacking	5.47	-5.179	3
		1	TYR 884	H-bonding	2.39		
		1	ASN 879	H-bonding	1.94		
		1	GLU 902	H-bonding	2.22		
	Palauamine	1	GLU 906	H-bonding	2.28	-4.942	2
		1	GLU 902	H-bonding	2.70		
		1	HIE 905	Pi-pi stacking	5.28		
		1	TYR 884	Pi-pi stacking	5.46		
Diazepinomicin	1	ASN 879	H-bonding	1.67	-4.747	1	
	1	HIE 905	Pi-pi stacking	3.92			
paenidigyamycin A	1	GLU 909	Salt-bridge	4.86	-4.66	0	
	1	GLU 906	Salt-bridge	3.99			
	1	HIE 905	Pi-pi stacking	4.08			
	1	IMD 1102	Pi-pi stacking	4.83			
	1	IMD 1102	Pi-pi stacking	4.99			
Oseltamivir	1	TYR 884	H-bonding	2.11	-4.764	1	
7AVT	hymenocardine-H	1	ASP 887	H-bonding	1.51	-5.866	2
		1	TYR 884	H-bonding	2.04		
	Boldine	1	ASN 879	H-bonding	1.79	-5.364	2
		1	TYR 884	Pi-pi stacking	5.25		
	(+)-N-methylisococlaurine	1	GLU 906	H-bonding	1.79	-5.244	
	Diazepinomicin	1	GLU 909	H-bonding	2.25	-5.102	3
		2	GLU 906	H-bonding	1.61		
			GLU 906	H-bonding	1.69		
	Spongiacidin B	1	TYR 884	Pi-pi stacking	5.13	-5.095	1
	Longamide B	1	TYR 884	Pi-pi stacking	5.46	-4.915	1
		1	LEU 901	H-bonding	1.60		
	O-desmethylnummularine-R	1	TYR 884	Pi-pi stacking	5.50	-4.793	2
		1	ASN 879	H-bonding	1.89		
		1	TYR 884	H-bonding	2.57		
Palauamine	1	IMD 1102	Pi-pi stacking	5.05	-4.593	2	
	1	GLU 909	H-bonding	1.80			
	1	GLU 902	H-bonding	2.23			
Oseltamivir	1	GLU 902	H-bonding	2.09	-3.773	1	

Table S-6: Binding free energies of all docked complexes

Proteins	Compounds	MM-GBSA dG Bind	MM-GBSA dG Bind Coulomb	MMGBSA dG Bind vdW	MMGBSA dG Bind Lipo
6UX9	(+)-N-methylisococlaurine	-69.99	-20.77	-41.78	-29.15
	oseltamivir	-66.66	-12.51	-49.61	-20.82
	spongiacidin B	-49.15	-23.68	-36.2	-11.08
	diazepinomicin	-76.73	-22.14	-58.29	-29.3
	Boldine	-66.4	-19.52	-40.59	-28.21
	longamide B	-52.04	-14.7	-35.81	-10.49
	palauamine	-50.67	-28.05	-40.04	-14.9
	Carpaine	-35.97	-2.29	-47.29	-15.29
7JX2	(+)-N-methylisococlaurine	-70.2	-0.14	-43.66	-32.72
	diazepinomicin	-80.96	-6.92	-63.82	-41.21
	Longamide B	-42.81	-20.46	-32.42	-9.18
	Spongiacidin B	-36.37	-1.07	-32.32	-11.38
	Boldine	-71.42	4.45	-56.34	-36.8
	oseltamivir	-54.32	0.58	-50.06	-20.26
6SFR	(+)-N-methylisococlaurine	-34.89	-4.1	-25.72	-16
	Spongiacidin B	-26.51	-0.55	-32.61	-9.39
	Boldine	-37.41	6.95	-36.56	-21.15
	Longamide B	-36.03	-7.81	-31.27	-6.57
	O-desmethylnumularine-R	-35.37	-7.83	-47	-17.02
	palauamine	-8.73	-11.96	-35.03	-11.01
	oseltamivir	-35.22	-9.58	-30.66	-11.13
	diazepinomicin	-26.83	4.13	-37.67	-16.7
	paenidigyamycin A	-60.21	-4.13	-45.9	-22.64
	hymenocardine-H	-26.48	-35.14	-34.46	-8.71
	Carpaine	-24.89	-14.29	-35.61	-12.94
6W81	hymenocardine-H	-72.59	-49.52	-55.22	-18.27
	(+)-N-methylisococlaurine	-51.04	-23.72	-30.75	-14.91

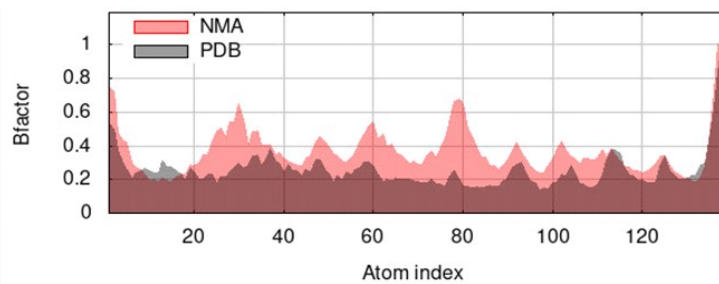
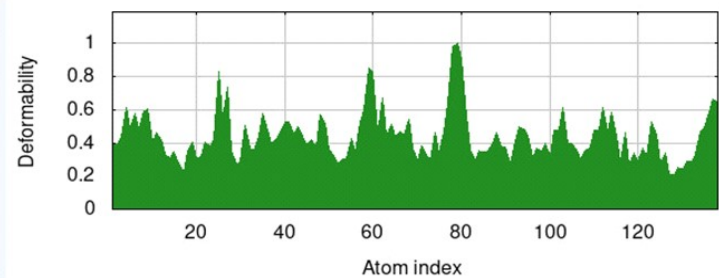
	palauamine	-57.48	-34	-24.74	-9.24
	Boldine	-51.9	-17.83	-39.46	-14.46
	spongiacidin B	-45.22	-39.16	-46.28	-5.07
	Diazepinomicin	-44.6	-9.68	-45.96	-11.23
	paenidigyamycin A	-66.97	-67.5	-56.87	-20.51
	longamide B	-30.37	-28	-19.14	-3.13
	O-desmethylnummularine-R	-57.79	-14.7	-57.81	-20.47
	oseltamivir	-45.46	-28.73	-22.36	-7.07
	Carpaine	-53.52	-15.97	-57.61	-13.45
7AVT	hymenocardine-H	-34.93	-11.49	-45.02	-15.48
	Boldine	-44.27	-18.45	-35.48	-19.24
	(+)-N-methylisococlaurine	-37.42	-20.09	-28.63	-15.67
	diazepinomicin	-35.34	-9.9	-35.07	-13.26
	Spongiacidin B	-30.89	-2.5	-34.18	-9.37
	Longamide B	-35.38	-15.9	-33.84	-6.08
	O-desmethylnummularine-R	-46.9	-17.78	-44.33	-16.49
	palauamine	-24.5	-15.04	-33.79	-9.94
	paenidigyamycin A	-63.86	-1.99	-44.68	-24.34
	oseltamivir	-37.82	-15.55	-34.24	-12.43
6W8H	Diazepinomicin	-69.55	-21.57	-50.64	-19.84
	Boldine	-67.73	-19.07	-37.23	-26.06
	(+)-N-methylisococlaurine	-62	-19.18	-35.87	-23.65
	palauamine	-56.84	-29.8	-40.38	-13.48
	spongiacidin B	-43.16	-32.55	-43.44	-12.61
	paenidigyamycin A	-64.33	42.83	-51.82	-31.39
	longamide B	-39.52	-0.95	-33.67	-8.1
	oseltamivir	-39.85	-13.44	-35.58	-16.51
	O-desmethylnummularine-R	-57.96	-3.62	-54.34	-22.26
	hymenocardine-H	-55.53	-8.24	-53.3	-20.84
	Carpaine	-48.85	9.19	-45.77	-17.43
6YNE	diazepinomicin	-71.21	-34.78	-21.03	-37.66

	palauamine	-43.83	-21.13	-7.96	-33.61
	(+)-N-methylisococlaurine	-42.87	-27.05	-14.99	-27.25
	spongiacidin B	-31.4	-17.19	-6.3	-25.02
	Boldine	-46.89	-17.36	-13.93	-27.83
	longamide B	-33.73	-19.62	-4.21	-22.53
	oseltamivir	-40.27	-18.83	-9.35	-31.26
	hymenocardine-H	-49.46	-25.18	-12.46	-44.83
	paenidigyamycin A	-46.35	63.19	-17.05	-38.19
	Carpaine	-35.69	-6.93	-8.71	-31.9
	O-desmethylnummularine-R	-23.78	7.61	-8.59	-34.51
7JVY	Diazepinomicin	-70.98	-3.51	-52.13	-38.75
	Boldine	-47.49	14.22	-36.44	-25.09
	(+)-N-methylisococlaurine	-41.19	14.45	-32.16	-24.12
	spongiacidin B	-25.99	-0.97	-25.93	-2.2
	longamide B	-25.68	-15.88	-10.3	0.82
	oseltamivir	-38.17	-3.27	-27.9	-10.43
7JWD	Diazepinomicin	-68.22	3.69	-56.3	-35.85
	Boldine	-64.23	-12.84	-47.01	-32.3
	(+)-N-methylisococlaurine	-58.51	2.69	-50.06	-31.52
	spongiacidin B	-43.11	-4.68	-41.35	-10.45
	longamide B	-50.73	4.63	-47.27	-10.2
	oseltamivir	-60.98	-8.77	-49.02	-18.57
6VF1	(+)-N-methylisococlaurine	1641.94	-4.31	462.43	-22.64
	boldine	125.75	5.16	9.08	-21.17
	carpaine	1389.57	77.14	426.37	-3.16
	diazepinomicin	91.49	20.42	1.64	-17.97
	hymenocardine-H	439.83	28.98	127.17	-18.54
	longamide B	78.69	10.16	-7.91	-6.62
	O-desmethylnummularine-R	85.46	-0.6	14.64	-28.38
	oseltamivir	46.24	46.05	-8.71	-12.79
	paenidigyamycin A	3293.07	216.57	1011.98	-24.2

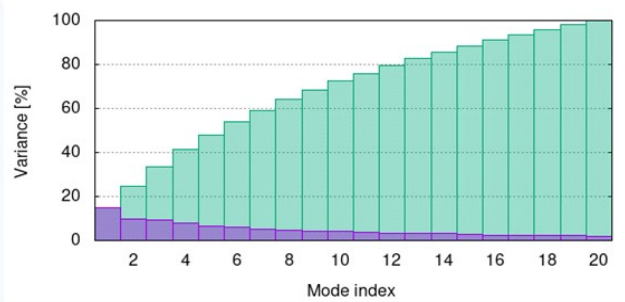
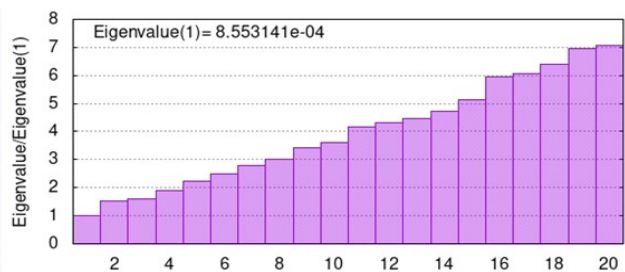
7JWR	palauamine	2155.23	12.36	593.8	-10.78
	spongiacidin B	20.97	-9.98	3.07	-5.18
	Diazepinomicin	-67.53	0.2	-54.92	-31.57
	Boldine	-74.74	-6.01	-45.14	-33.36
	(+)-N-methylisococlaurine	-69.66	-11.13	-40.87	-33.02
	spongiacidin B	-44.14	-22.01	-35.27	-12.63
	longamide B	-52.3	-14.33	-43.73	-11.14
	oseltamivir	-58.5	-3.43	-49.87	-21.18

Table S-7: ADMET Pharmacokinetic Properties of the top three compounds

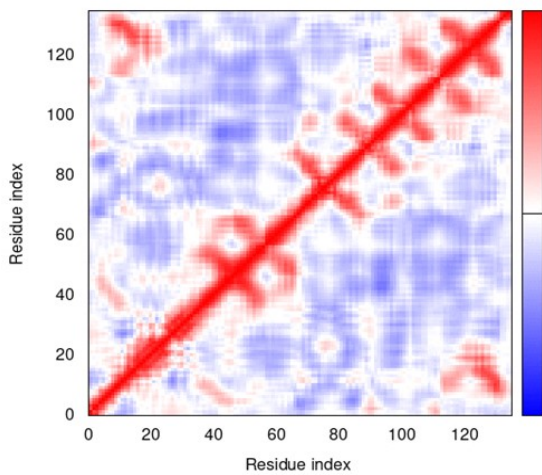
Variant	CNS	mol MW	Donor HB	Accept HB	logP	logS	QPPCaco	QPlogBB	QPPMDCK	logKp	QPlogKhsa	Percent Human Oral Absorption	Rule Of Five
(+)-N-methylisococlaurine	1	299.369	2	4.25	32.19	-2.912	244.511	-0.312	119.413	-4.353	0.238	84.536	0
Diazepinomicin	-2	462.588	4	5.75	50.627	-7.244	209.925	-2.13	91.534	-2.957	0.943	100	0
hymenocardine-H	-2	653.82	2.75	14	65.658	-3.908	96.477	-1.057	71.97	-4.162	-0.703	46.753	2



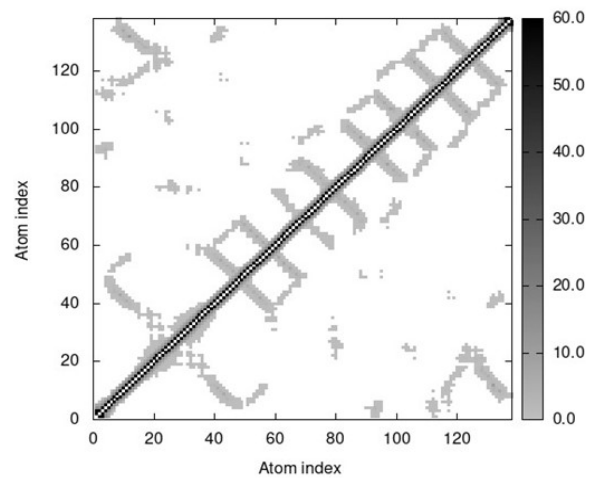
(A)



(B)



(C)



(D)

Figure S1: results of MD stimulation (A) Deformability and B-factor, (B) Eigenvalue and variance, (C) residue index, (D) atom index of 7JWR-diazepinomicin

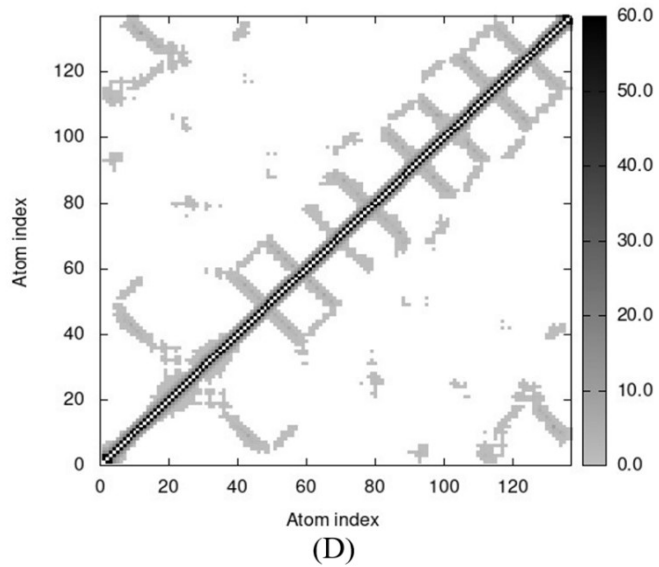
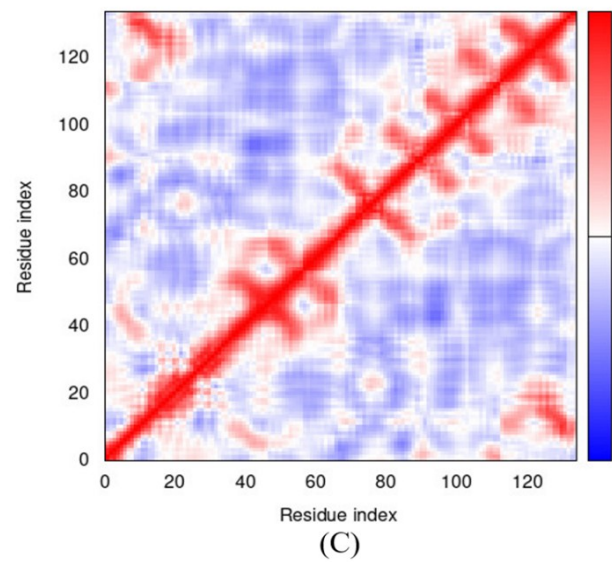
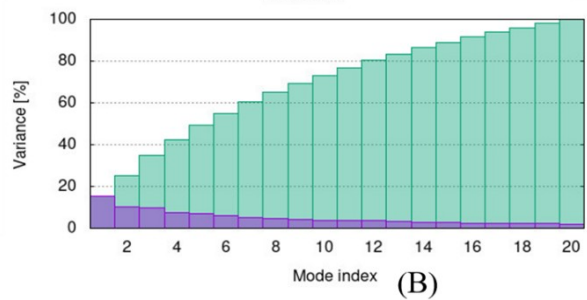
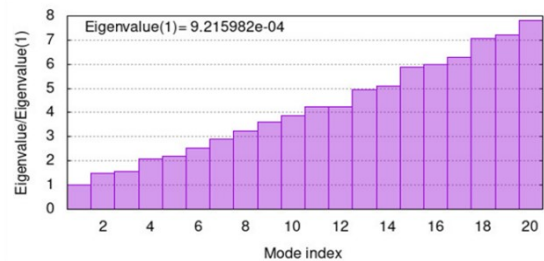
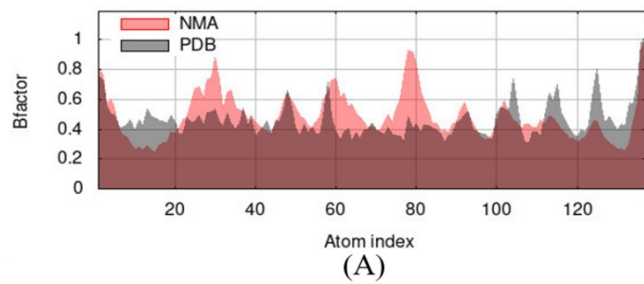
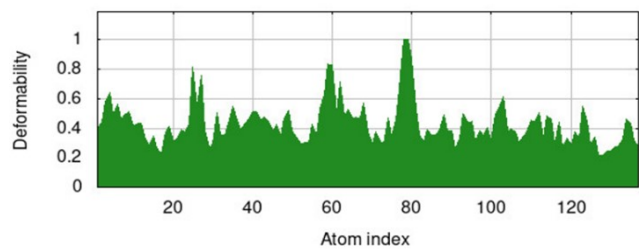
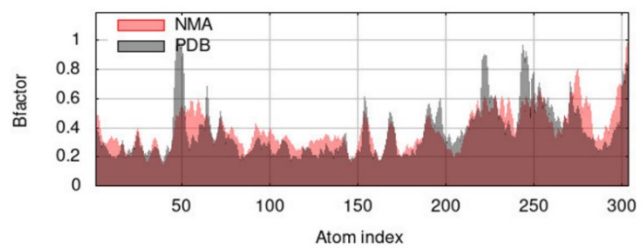
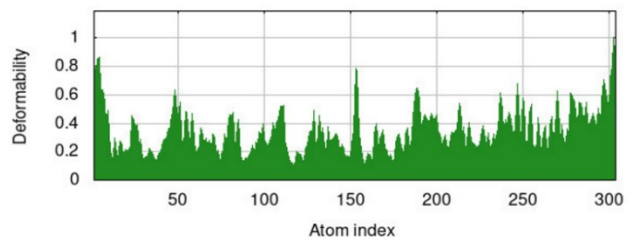
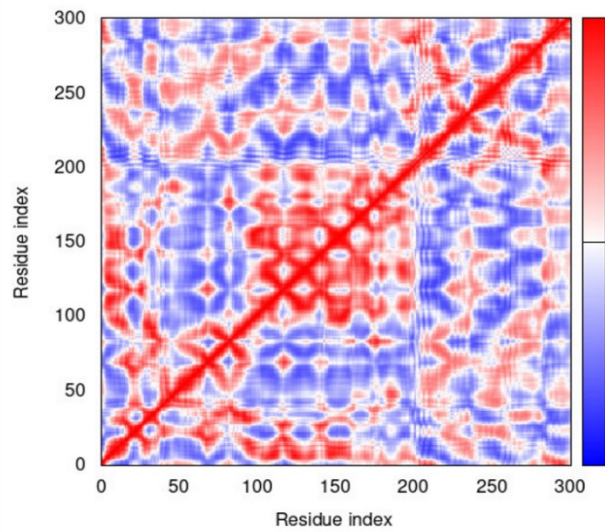
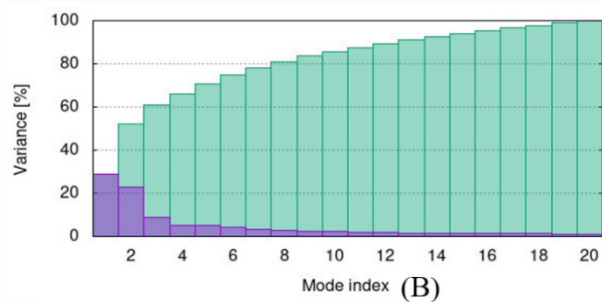
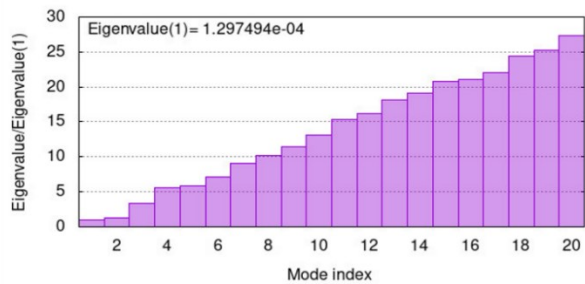


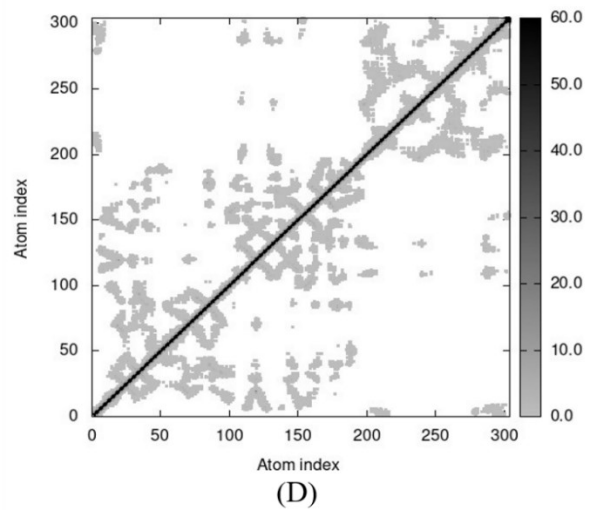
Figure S2: results of MD stimulation (A) Deformability and B-factor, (B) Eigenvalue and variance, (C) residue index, (D) atom index of 7JX2-(+)-N-methylisococlaurine



(A)



(C)



(D)

Figure S3: results of MD stimulation (A) Deformability and B-factor, (B) Eigenvalue and variance, (C) residue index, (D) atom index of 6W81- hymenocardine-H